Available online at www.sciencedirect.com
SCIENCE DIRECT®
Bioorganic & Medicinal Chemistry 12 (2004) 5661–5675
Bioorganic & Medicinal Chemistry

Design and synthesis of highly potent and selective (2-arylcarbamoyl-phenoxy)-acetic acid inhibitors of aldose reductase for treatment of chronic diabetic complications

Michael C. Van Zandt,[a,*] Evelyn O. Sibley,[a] Erin E. McCann,[a] Kerry J. Combs,[a] Brenda Flam,[a] Diane R. Sawicki,[a] Al Sabetta,[a] Anne Carrington,[a] Janet Sredy,[a] Eduardo Howard,[b] Andre Mitschler[b] and Alberto D. Podjarny[b]

[a]*The Institute for Diabetes Discovery, LLC, 23 Business Park Drive, Branford, CT 06405, USA*
[b]*Laboratoire de Biologie et Genomique Structurales, UPR 9004 du CNRS, IGBMC, 1 rue Laurent Fries, B.P. 163, 67404 Illkirch Cedex, France*

Received 14 May 2004; revised 28 July 2004; accepted 28 July 2004
Available online 1 September 2004

Abstract—Recent efforts to identify treatments for chronic diabetic complications have resulted in the discovery of a novel series of highly potent and selective (2-arylcarbamoyl-phenoxy)-acetic acid aldose reductase inhibitors. The compound class features a core template that utilizes an intramolecular hydrogen bond to position the key structural elements of the pharmacophore in a conformation, which promotes a high binding affinity. The lead candidate, example **40**, 5-fluoro-2-(4-bromo-2-fluoro-benzylthiocarbamoyl)-phenoxyacetic acid, inhibits aldose reductase with an IC_{50} of 30 nM, while being 1100 times less active against aldehyde reductase, a related enzyme involved in the detoxification of reactive aldehydes. In addition, example **40** lowers nerve sorbitol levels with an ED_{50} of 31 mg/kg/d po in the 4-day STZ-induced diabetic rat model.

1. Introduction

Diabetes mellitus and its disabling complications, which include blindness, renal failure, neuropathy, limb amputation, myocardial infarction, and stroke affect some 17 million people in the United States with an estimated cost of over 100 billion dollars annually.[1] Through various clinical studies, including the Diabetes Control and Complications Trial (DCCT) and the United Kingdom Prospective Diabetes Study (UKPDS), the development and progression of these complications in type I and type II patients has been clearly linked to elevated blood glucose levels.[2,3] During euglycemic conditions glucose is preferentially metabolized through the glycolytic pathway where it is phosphorylated with ATP by hexokinase to form glucose-6-phosphate. However, during conditions of hyperglycemia, as observed in diabetes mellitus, elevated blood glucose levels saturate the normal pathways of glucose metabolism and a dramatic increase in flux through the polyol pathway results (Scheme 1). Glucose entering the polyol pathway is reduced to sorbitol by aldose reductase (ALR2) and NADPH. Sorbitol is subsequently oxidized to fructose by sorbitol dehydrogenase and NAD^+. This increased flux through the polyol pathway results in a change in redox potential for these cofactors. The increased ratio of cytosolic NADH to NAD^+ is called reductive stress, which has been linked to depleted intracellular levels of glutathione, increased nonenzymatic glycation, and activation of protein kinase C.[4,5] In addition to reductive stress, accumulation of sorbitol in certain cells results in osmotic stress, which can lead to cell swelling and eventually cell death.[6] Inhibitors of aldose reductase can prevent these metabolic and biochemical changes, which have been linked to the pathogenesis of diabetic complications.[7]

In addition to these biochemical endpoints, recent reports provide a strong genetic correlation between over expression of aldose reductase and the development of diabetic complications.[8–10] As a result, a high ALR2

Keywords: Aldose reductase; Aldehyde reductase; Diabetes; Complications.
* Corresponding author. Tel.: +1 203 315 5951; fax: +1 203 315 4002; e-mail: michael.vanzandt@ipd-discovery.com

0968-0896/$ - see front matter © 2004 Elsevier Ltd. All rights reserved.
doi:10.1016/j.bmc.2004.07.062

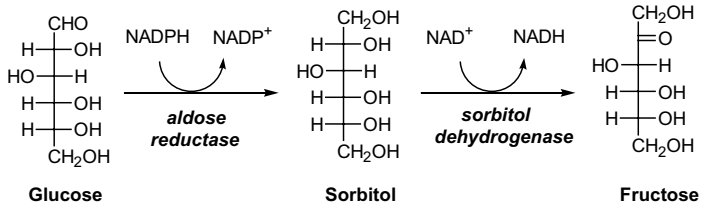

Scheme 1. Polyol pathway.

level is now considered to be an important risk factor for chronic diabetic complications including neuropathy, retinopathy, and nephropathy.

Although many potent aldose reductase inhibitors (ARIs) have been identified and developed, none are currently marketed for worldwide use.[4,7] Many of these candidates failed to gain acceptance due to an inadequate therapeutic index. In some cases this toxicity may have resulted from a lack of selectivity relative to aldehyde reductase (ALR1). The physiological importance of ALR1 has been clearly demonstrated.[11,12] It converts highly reactive 2-oxoaldehydes like 3-deoxyglucosone and methyl glyoxal to their corresponding nonreactive alcohols.[13,14] These aldehydes, which are involved in the formation of various protein cross-links and other advanced glycation end products (AGEs), are formed as degradation products from glucose and fructose.[15] During conditions of prolonged hyperglycemia, high concentrations of these aldehydes are formed resulting in the development of chronic diabetic complications and accelerated aging.[16–18]

As a member of the aldo-ketoreductase super family, ALR1 shares greater than 85% homology with ALR2 (rat and man).[19] Specific amino acid changes in the C-terminal loop, a section of the protein lining the active site cleft, are responsible for various substrate and inhibitor specificities.[20]

Efforts to design novel, potent, and selective ARIs have resulted in the discovery of a compound class that features a 2-arylcarbamoyl-phenoxyacetic acid as a core template. Within this template, an intramolecular hydrogen bond is used to position the acetic acid moiety and aromatic side chain, the key structural elements of the pharmacophore, in the necessary orientation for high binding affinity.

2. Inhibitor design and synthesis

The target compounds were synthesized using methods illustrated in Schemes 2–4. (2-Arylcarbamoyl-phenoxy)-acetic acids **6**, **8**, and **13** in Scheme 2 illustrate methods used to prepare most examples. Treatment of commercially available 2,4-difluorobenzoic acid (**1**) with sodium hydroxide at 135 °C affords 4-fluorosalicyclic acid.[21] Activation of the carboxylic acid with thionyl chloride provides the corresponding acid chloride, which is coupled with 3-nitrobenzylamine to give amide **4**. Alkylation with ethyl bromoacetate followed by hydro-

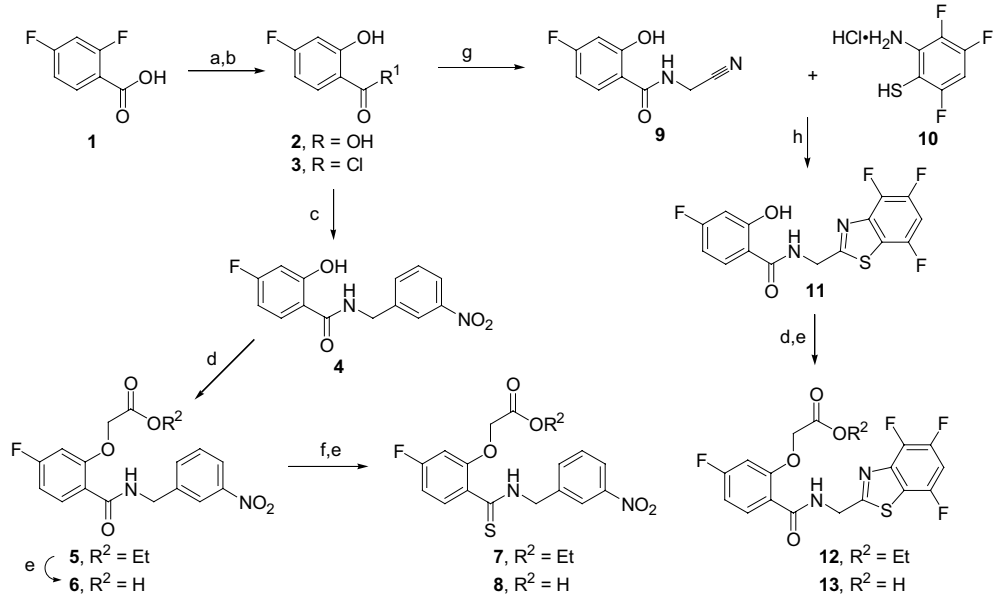

Scheme 2. Reagents and conditions: (a) NaOH, DMI, 135 °C (68%); (b) $SOCl_2$, cat. DMF, heptane, 60 °C, (85%); (c) 3-nitrobenzylamine, TEA, CH_2Cl_2 (67%); (d) ethyl bromoacetate, aq K_2CO_3, acetone; (e) aq NaOH, ethanol; (f) P_4S_{10}, pyridine (98%); (g) aminoacetonitrile hydrochloride, TEA, CH_2Cl_2 (65%); (h) ethanol, heat (21%).

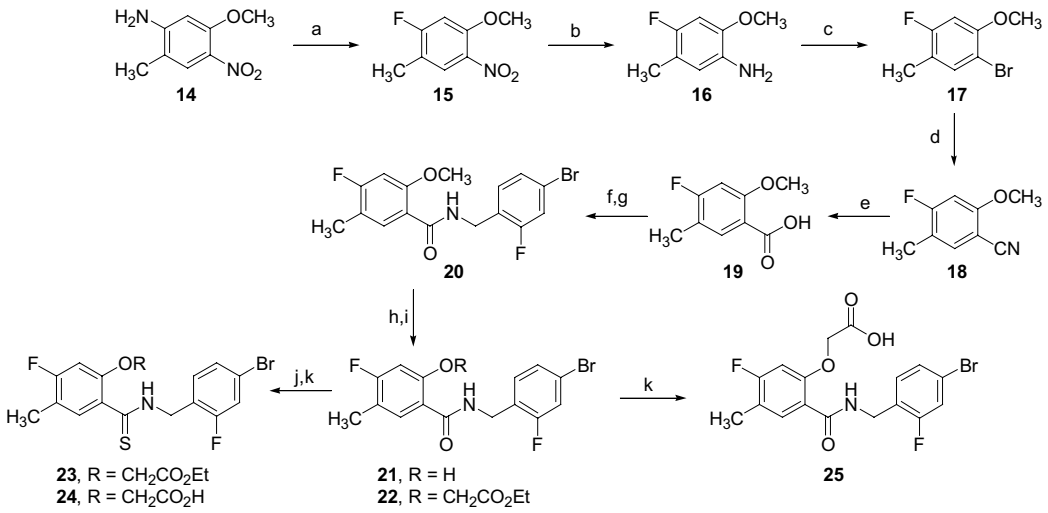

Scheme 3. Reagents and conditions: (a) $NaNO_2$, HF-pyridine (76%); (b) H_2, 10% Pd–C, ethanol (99%); (c) 48% aq HBr, $NaNO_2$, CuBr (47%); (d) CuCN, DMF, 160 °C (86%); (e) 2 N NaOH, 90 °C, (96%); (f) $(COCl)_2$, cat. DMF, CH_2Cl_2; (g) 4-bromo-2-fluorobenzylamine hydrochloride, DIEA, CH_2Cl_2 (97%, two steps); (h) 25% aq HBr, AcOH, 120 °C (73%); (i) ethyl bromoacetate, aq K_2CO_3, acetone (93%); (j) P_4S_{10}, pyridine (89%); (k) aq NaOH, ethanol.

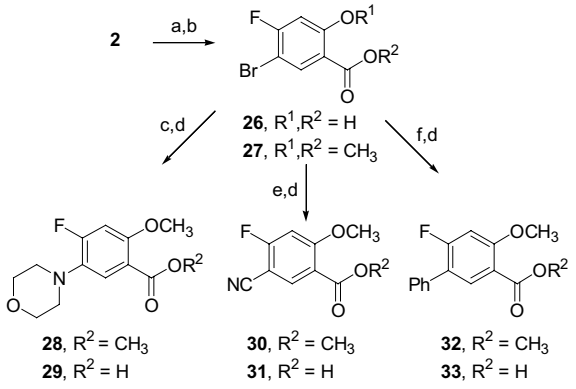

Scheme 4. Reagents and conditions: (a) Br_2, AcOH, H_2SO_4 (95%); (b) CH_3I, K_2CO_3, acetone (80%); (c) morpholine, Cs_2CO_3, $Pd(OAc)_2$, BINAP, toluene, 100 °C (47%); (d) aq NaOH, ethanol; (e) CuCN, DMF, 150 °C (75%); (f) $PhB(OH)_2$, K_2CO_3, $Pd(PPh_3)_4$, toluene, 110 °C (91%).

lysis of the ethyl ester gives phenoxyacetic acid **6**. Alternatively, treatment of amide **5** with phosphorous pentasulfide followed by hydrolysis provides thioamide derivative **8**. If the benzothiazole derivatives are desired, aminoacetonitrile can be used in place of the substituted benzylamine to provide nitrile **9**, which can subsequently be condensed with the desired 2-aminothiophenol (**10**) to provide amide **11**. Alkylation of the phenol with ethyl bromoacetate followed by hydrolysis of the ethyl ester provides the target benzothiazole derivative **13** in high yield.

Additional examples, where the desired substituted salicylic acid or corresponding 2-fluorobenzoic acid starting materials were not commercially available, were prepared separately and are described in Schemes 3 and 4. The 2-fluoro-3-methyl examples were prepared using chemistry outlined in Scheme 3.

Diazotization of commercially available 5-methoxy-2-methyl-4-nitroaniline (**14**) with sodium nitrite in the presence of HF-pyridine provided the corresponding fluoride[22] (**15**) in 76% yield. Subsequent hydrogenation followed by diazotization and treatment with a CuBr provided bromide **17**.[23] Treatment with CuCN in DMF at 160 °C gave nitrile **18** (86%), which was hydrolyzed with aq NaOH to give carboxylic acid **19**. Formation of the acid chloride with oxalyl chloride and catalytic DMF followed by coupling with 4-bromo-2-nitrobenzylamine provided amide **20** in nearly quantitative yield. Deprotection of the methyl ether with 25% HBr in acetic acid at 120 °C followed by alkylation with ethyl bromoacetate and hydrolysis provides target amide **25**. Alternatively, treatment of ester **22** with phosphorous pentasulfide and subsequent hydrolysis provides the corresponding thioamide target (**24**).

The syntheses of additional 4-fluoro analogs with other substituents in the 5-position were conveniently prepared via bromide **26** as illustrated in Scheme 4. Bromination of 4-fluorosalicyclic acid with Br_2 in a solution of acetic acid and sulfuric acid followed by alkylation with iodomethane and aq K_2CO_3 provided the bis-alkylated intermediate **27** in 76% yield (two steps). This highly functionalized salicylic acid intermediate was used to prepare examples with a variety of substituents in the 4-position. For example, the morpholine intermediate **28** was prepared from bromide **27** using standard Bückwald conditions.[24] The nitrile intermediate **30** was prepared by treating bromide **27** with CuCN in DMF at 150 °C (75%). Additionally, a Suzuki coupling of phenylboronic acid with bromide **27** provided phenyl derivative **32**. These intermediates were used to prepare the corresponding target compounds using methods already described in Schemes 2 and 3.

3. Results and discussion

The major objective of this program has been to identify highly potent, selective and efficacious aldose reductase inhibitors for treatment of chronic diabetic complications. All compounds in the program were initially tested for potency against human aldose reductase (hALR2) and selectivity relative to human aldehyde reductase (hALR1). Selected compounds with significant in vitro activity against hALR2 were also tested in the 4-day streptozotocin (STZ) induced diabetic rat model. The results from these experiments are listed in Tables 1–3.

The program benefited significantly from the early use of X-ray crystallography. The structures provided a clear understanding of the important interactions that make up the enzyme-inhibitor complexes. This information was used to identify the specific fragments of the inhibitor template that provided the greatest opportunities for optimization of potency and selectivity relative to aldehyde reductase.

The complexes were obtained using hALR2 expressed in *E. coli* and crystallized with the oxidized form of the coenzyme β-$NADP^+$ at pH 5 and 277 K. Initial results with example **40** provided a clear picture of the inhibitor-enzyme complex (1.8 Å). As illustrated in Figure 1, the inhibitor is oriented in the active site of hALR2 in a manner such that the hydrophilic carboxylate head forms tight hydrogen bonds with the OH of Tyr 48 (2.74 Å), the NE2 of His 110 (2.67 Å), and the NE1 of Trp 111 (3.07 Å). The carboxylate also forms an optimal intramolecular hydrogen bond (3.01 Å) with the amide N–H forming a unique nine-membered ring. In addition to the hydrogen bonding interactions, the benzyl side chain forms a nearly perfect π-stacking interaction with the indole moiety of Trp 111. These interactions anchor the inhibitor deep within the enzyme active site.

As this class of inhibitors bind to the hALR2 active site, a conformational change occurs opening a pocket localized between Phe 122, Trp 111, Leu 300, and Ala 299.[25] The specific opening of the pocket varies to accommodate each inhibitor, producing an 'induced fit'. Since the residues lining this pocket are not conserved in aldehyde reductase, the interactions are specific for ALR2.[26–28] As a result, inhibitors with binding interactions in this 'specificity pocket' are generally highly selective for aldose reductase. The specific interactions within the specificity pocket, for example, **40** include a significant π-stacking interaction of the benzyl side chain with the indole moiety of Trp 111, H-bonding interactions between the side chain fluorine and amide N-H's of Leu 300 (3.30 Å) and Ala 299 (3.27 Å), and an unusually short contact between the benzyl Br and Thr 113-OG (2.98 Å). This Br-Thr-OG interaction is likely important for selectivity since in aldehyde reductase Thr 113 is replaced by a much bulkier tyrosine, which would cause steric hindrance.

After significant optimization, subsequent co-crystallization experiments with example **40** have resulted in a new, more refined, structure with exceptional resolution (0.66 Å). These results will undoubtedly advance our understanding of the catalytic mechanism. The details of this work has been published separately.[29]

With a clear picture of the inhibitor-enzyme complex early in the lead optimization program, little was done with the (2-arylcarbamoyl-phenoxy)-acetic acid core structure. New analog synthesis was primarily directed to those areas perceived to have the greatest potential for significant improvement. In keeping with our belief that selectivity relative to aldehyde reductase would play an important role in the success of any clinically useful ARI, a significant portion of the optimization effort was directed toward the aromatic side chain. The side chain is the portion of the inhibitor that interacts with the C-terminal loop, the region of the enzyme most differentiated between hALR2 and hALR1. In general, the structure–activity relationships associated with the structural class are consistent with binding information derived from the enzyme-inhibitor complexes. Large variations in hALR2 activity are observed with different substitution patterns on the aromatic side chain. In general, the compounds with the strongest binding affinities contained electron deficient aromatic side chains. All examples with strong electron donating substituents had poor binding affinities with IC_{50}'s > 2 μM (**35**, 7-methoxy; **43**, 6,7-methylenedioxo; **50**, 6,8-dimethoxy). Examples with substituents only in the *para*-position (R_7) were, at best, only weakly active with Br being preferred with an IC_{50} of 550 nM (**37**, Br > **41**, Cl > **34**, H > **35**, OCH_3 > **36**, CF_3). Addition of an *ortho*- or *meta*-substituent often provides a dramatic increase in potency. This is illustrated in example **42** where introduction of a second chlorine (6,7-dichloro), results in an IC_{50} of 34 nM. This is nearly a 40-fold increase in potency relative to example **41** (7-choro), which has an IC_{50} of 1300 nM. A similar effect is observed when comparing example **37** (7-bromo) with example **38** (5-fluoro-7-bromo). Introduction of the 5-fluoro group brings the IC_{50} from 550 to 30 nM, nearly a 20-fold increase in potency. In general, electron withdrawing groups capable of being hydrogen bond acceptors in the *ortho* or *meta*-positions appear to be critical for high in vitro potency. Preferred substituents include fluorine, trifluoromethyl, and nitro. The IC_{50}'s for examples with a 6-fluoro (**46**), 6-trifluoromethyl (**47**), and 6-nitro (**44**) are 820, 39, and 6 nM, respectively. Introduction of second *meta*-substituted group can provide some improvement as seen in example **48**, with a 6-triflouromethy and 8-fluoro-substituent, which has an IC_{50} of 29 nM. All activity is lost however when two large trifluormethyl substituents are present in the *meta*-positions as seen in example **49** with an IC_{50} of only 22 μM. In this example, the side chain is simply too large for the specificity pocket.

As consistent with previously identified ARIs, the preferred substitution patterns appear to be the 3-nitro benzyl (**8**) and the 2-fluoro-4-bromo benzyl (**40**).[30,31] These examples are highly potent and selective with IC_{50}'s of 6 and 30 nM for hALR2 and 35,000 and 33,000 nM for hALR1, respectively.

Table 1. Physical and in vitro inhibitory properties of (2-benzylcarbamoyl-phenoxy)-acetic acid ARIs

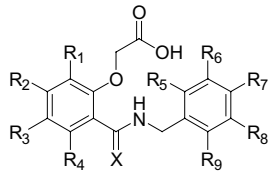

Ex.	Substituents	X	Mp (°C)	Empirical formula	Analysis	Inh. IC_{50} (nM)	
						hALR2	hALR1
34	2-Cl	O	145–146	$C_{16}H_{14}ClNO_4$	C, H, N, Cl	3300	NT[a]
35	2-Cl, 7-OCH_3	O	178–179	$C_{20}H_{22}ClNO_5$	C,[b] H, N, Cl	8800	NT
36	2-Cl, 7-CF_3	O	184–185	$C_{17}H_{13}ClF_3NO_5$	C,[b] H, N, Cl[b]	10,000	NT
37	2-Cl, 7-Br	O	172–173	$C_{16}H_{13}BrClNO_4$	C, H,[b] N, Cl	550	NT
38	2-Cl, 5-F, 7-Br	O	184–185	$C_{16}H_{12}BrClFNO_4$	C, H, N, Cl	30	14,000
39	2-F, 5-F, 7-Br	O	143–145	$C_{16}H_{12}BrF_2NO_4$	C, H, N	55	6600
40	2-F, 5-F, 7-Br	S	154–157	$C_{16}H_{12}BrF_2NO_3S$	C, H, N, S, Br	30	33,000
41	2-Cl, 7-Cl	O	184–186	$C_{16}H_{13}Cl_2NO_4$	C, H, N, Cl	1300	NT
42	2-Cl, 6-Cl, 7-Cl	O	177–178	$C_{16}H_{12}Cl_3NO_4$	C, H, N, Cl	34	18,000
43	2-Cl, 3-4-methylenedioxo	O	208–209	$C_{17}H_{14}ClNO_6$	C, H, N, Cl	2800	NT
44	2-Cl, 6-NO_2	O	200	$C_{16}H_{13}ClN_2O_6$	C, H, N, Cl	6	NT
6	2-F, 6-NO_2	O	148–151	$C_{16}H_{13}FN_2O_6$	C, H, N	8	34,000
8	2-F, 6-NO_2	S	147–150	$C_{16}H_{13}FN_2O_5S$	C, H, N	6	35,000
45	2-F, 6-NO_2, 7-CH_3	O	159–160	$C_{17}H_{15}FN_2O_6$	C, H, N	8	5000
46	2-Cl, 6-F	O	155	$C_{16}H_{13}ClFNO_4{\cdot}H_2O$	C, H,[b] N, Cl	820	NT
47	2-Cl, 6-CF_3	O	179–181	$C_{17}H_{15}ClF_3NO_4$	C, H, N, Cl	39	6700
48	2-Cl, 6-CF_3, 8-F	O	160–162	$C_{17}H_{12}ClF_4NO_2$	C, H, N, Cl	29	7300
49	2-Cl, 6-CF_3, 8-CF_3	O	191–193	$C_{18}H_{12}ClF_6NO_4$	C, H, N, Cl	22,000	NT
50	2-Cl, 6-OCH_3, 8-OCH_3	O	163	$C_{18}H_{18}ClNO_6$	C, H, N, Cl	4800	NT
51	2-Cl, 5-F, 9-F	O	189–191	$C_{16}H_{12}ClF_2NO_2$	C, H, N	730	NT
52	5-F, 7-Br	O	144–145	$C_{16}H_{13}BrFNO_4$	C, H, N	176	2400
53	2-CH_3, 5-F, 7-Br	O	188–189	$C_{17}H_{15}BrFNO_4$	C, H, N	630	NT
54	2-CF_3, 5-F, 7-Br	O	169–170	$C_{17}H_{12}BrF_4NO_4$	C, H, N	2,400	NT
55	2-OCH_3, 5-F, 7-Br	O	203–204	$C_{17}H_{15}BrFNO_5$	C, H, N	550	NT
56	2-SCH_3, 5-F, 7-Br	O	196–199	$C_{17}H_{15}BrFNO_4S$	C, H, N, S	83	2900
57	2-SO_2CH_3, 5-F, 7-Br	O	193–194	$C_{17}H_{15}BrFNO_6S$	C,[b] H, N, S	13,000	NT
58	2-F, 3-F, 5-F, 7-Br	O	156–158	$C_{16}H_{11}BrF_3NO_4$	C, H, N	37	1100
59	2-F, 3-F, 5-F, 7-Br	S	206–209	$C_{16}H_{11}BrF_3NO_3S$	C, H, N, S	33	2700
25	2-F, 3-CH_3, 5-F, 7-Br	O	169	$C_{17}H_{14}BrF_2NO_4$	C, H, N	24	5900
24	2-F, 3-CH_3, 5-F, 7-Br	S	162–164	$C_{17}H_{14}BrF_2NO_3S$	C, H, N, S	24	31,000
60	2-F, 4-F, 5-F, 7-Br	O	158–159	$C_{16}H_{11}BrF_3NO_4$	C, H, N	820	11,000
61	3-F, 5-F, 7-Br	O	145–146	$C_{16}H_{10}BrFNO_4$	C, H, N	150	5500
62	3-Br, 5-F, 7-Br	O	153–155	$C_{16}H_{12}Br_2FNO_4$	C, H, N, Br	64	1800
63	3-Br, 5-F, 7-Br	S	153–155	$C_{16}H_{12}Br_2FNO_3S$	C, H, N, Br, S	37	1900
64	3-CH_3, 5-F, 7-Br	O	145–146	$C_{17}H_{15}BrFNO_4$	C, H, N	69	11,000
65	3-NH_2, 5-F, 7-Br	O	204 dec	$C_{16}H_{14}BrFN_2O{\cdot}0.5H_2O$	C, H, N	8300	NT
66	3-NO_2, 5-F, 7-Br	O	174–175	$C_{16}H_{12}BrFN_2O_6$	C, H, N	200	7900
67	3-NHAc, 5-F	O	235 dec	$C_{18}H_{17}FN_2O_5$	C, H, N	5000	NT
68	3-OH, 5-F, 7-Br	O	244 dec	$C_{16}H_{13}BrFNO_5$	C, H, N	470	NT
69	3-OCH_3, 5-F, 7-Br	O	149–150	$C_{17}H_{15}BrFNO_5$	C, H, N	100	NT
70	3-$OCH_2CH_2CH_3$, 5-F, 7-Br	O	186–187	$C_{19}H_{19}BrFNO_5$	C, H, N	3100	NT
71	3-OCH_2CHCH_2, 5-F, 7-Br	O	182–183	$C_{19}H_{17}BrFNO_5$	C, H, N	2700	NT
72	1,2-Benzo, 5-F, 7-Br	O	163–165	$C_{20}H_{15}BrFNO_4$	C, H, N	>50 μM	NT
73	2,3-Benzo, 5-F, 7-Br	O	229–230	$C_{20}H_{15}BrFNO_4$	C, H, N	130	NT
74	3,4-Benzo, 5-F, 7-Br	O	189–190	$C_{20}H_{15}BrFNO_4$	C, H, N	1100	NT
75	2-F, 3-Br, 6-NO_2	O	169–172	$C_{16}H_{12}BrFN_2O_6$	C, H, N, Br	6	44,000
76	2-F, 3-morpholino, 6-NO_2	O	180	$C_{20}H_{20}FN_3O_7$	C, H, N	7	54,000
77	2-F, 3-CN, 6-NO_2	O	179–180	$C_{17}H_{12}FN_3O_6$	C, H, N	7	6500
78	2-F, 3-Ph, 6-NO_2	O	210–211	$C_{22}H_{17}FN_2O_6$	C, H, N	8	14,000
79	2-F, 3-Ph, 6-NO_2	S	177–179	$C_{22}H_{17}FN_2O_5S$	C, H, N	11	12,000
80	2-F, 3-CH_3, 6-NO_2	O	177–179	$C_{17}H_{15}FN_2O_6$	C, H, N	8	2600
81	2-F, 3-CH_3, 6-NO_2	S	137–139	$C_{17}H_{15}FN_2O_2S$	C, H, N, S	7	3100
82	3-CH_3, 6-NO_2	O	193–194	$C_{17}H_{16}N_2O_6$	C, H, N	11	NT
83	3-OCF_3, 6-NO_2	O	154–156	$C_{17}H_{13}F_3N_2O_7$	C, H	9	NT
84	3-OCF_3, 6-NO_2	S	158–161	$C_{17}H_{13}F_3N_2O_6S$	C, H, N, S	12	3600
85	2-F, 6-NO_2, N-CH_3	O	180–182	$C_{17}H_{15}FN_2O_6$	C, H, N	5300	NT
Tolrestat						14	1900

[a] Not tested.
[b] Elemental analysis not within ±4% of theoretical value.

Table 2. Physical and in vitro properties of {2-[(benzothiazol-2-ylmethyl)-carbamoyl]-phenoxy}-acetic acid ARIs

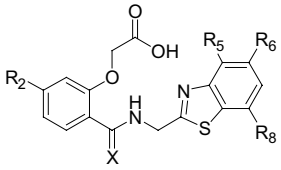

Ex.	Substituents	X	Mp (°C)	Empirical formula	Analysis	Inhibition IC_{50} (nM)	
						hALR2	hALR1
86	2-Cl, 6-CF_3	O	225–227	$C_{18}H_{12}ClF_3N_2O_4S$	C, H, N, Cl	35	8600
87	2-F, 6-CF_3	O	206–208	$C_{19}H_{13}F_4NO_4S$	C, H, N	29	35,000
13	2-F, 5-F, 6-F, 8-F	O	172–174	$C_{17}H_{10}F_4N_2O_4S$	C, H, N	11	22,000
88	2-F, 5-F, 6-F, 8-F	S	150	$C_{17}H_{10}F_4N_2O_3S_2$	NT[a]	15	17,000

[a] Not tested.

Table 3. In vivo activity of phenoxyacetic acid ARIs

Ex.	Inhibition of sorbitol accumulation in STZ-induced diabetic rat nerve		
	Dose (mg/kg/d) po	% Inh.	ED_{50} (mg/kg/d) po
38	50	33	
44	50	27	
52	50	15	
64	50	39	
39	50	54	
82	50	37	
6	50	41	
40	10	40	31
8	50	89	
25	50	49	
24	50	36	
87	50	16	
13	50	55	
88	50	62	
Tolrestat	10	31	

Substitution on the core salicylic acid structure is generally well tolerated and can significantly improve in vitro and in vivo activity. Exceptions include those examples with large groups in the 1 and 2-positions where unfavorable steric interactions occur with VAL 47 (examples **54**, **57**, and **72**). When comparing examples **39** and **52**, introduction of fluorine in the 2-position provides about a threefold increase in potency and selectivity. In vivo efficacy is also significantly increased with the 2-fluoro substituent. The 3-methyl derivative (**64**) also provided a significant improvement in potency, selectivity, and in vivo efficacy relative to the unsubstituted example (**52**). When combined together, the 2-fluoro-3-methyl derivative (**25**) provided an additive improvement relative to the monosubstituted examples in the primary in vitro assay. Unfortunately, the same effect was not observed in the in vivo model.

Examples with a nitro substituent in the *meta*-position on the benzyl ring (R_6) are consistently most potent in the primary in vitro assay. Some of the most interesting examples combine the 6-nitro substituent on the aromatic side chain with the 2-fluoro substituent on the salicylic amide moiety (examples **6**, **8**, **44**, **75**–**81**). Within this series a variety of substituents have been introduced in the 3-position. Examples **75** (R_3 = bromo) and **76** (R_3 = morpholino) are also two of the most selective with IC_{50}'s for hALR1 of 44,000 and 54,000 nM, respectively. With selectivity ratios (hALR1/hALR2) > 7000, these are among the most selective inhibitors identified to date. Other examples in this series including **77** (R_3 = cyano), **78** (R_3 = phenyl), **80** (R_3 = methyl), and the corresponding thioamide derivatives (**79** and **81**) are also very potent, but somewhat less selective.

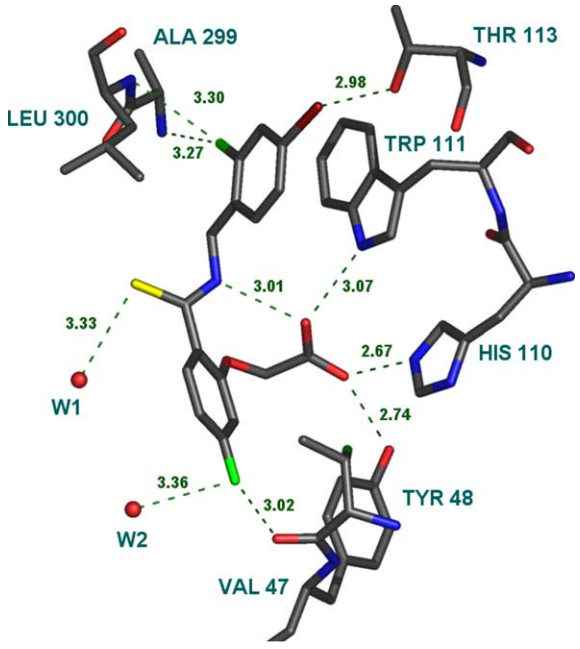

Figure 1. Environment of inhibitor example **40** in the subatomic resolution structure of aldose reductase. Contacts shorter than 3.5 Å are indicated. Note the short contacts of the inhibitor carboxylic acid head with residues Tyr 48, His 110, and Trp 111 and the perfect π-stacking of the benzyl side chain with the indole moiety of Trp 111.

In addition to the (2-benzylcarbamoyl-phenoxy)-acetic acids a few {2-[(benzothiazol-2-ylmethyl)-carbamoyl]-phenoxy}-acetic acids were also prepared (Table 2). In general the in vitro and in vivo activities were comparable to the benzyl series. Example **87** with a 2-fluoro substituent has similar potency for hALR2 as the corresponding example with the 2-chloro substituent (**86**), but is approximately fourfold more selective. When

comparing substituents on the benzthiazole, the 5,6,8-trifluoro example (**13**) is about twofold more potent and selective relative to the 6-trifluoromethyl example (**87**). The thioamide analog of example **13**, (**88**) is somewhat less potent and selective, but both have good activity in the STZ-diabetic rat model.

Because of the obvious importance in positioning the key elements of the pharmacophore, few modifications of the amide linker were explored. The *N*-methyl derivative, example **85**, is approximately 700-fold less active than the corresponding *N*–H derivative, example **6**. As expected, this indicates the intramolecular hydrogen bond between the phenolic ether and carboxylate is critical for activity. In contrast to the *N*-methyl derivative, a significant improvement in oral efficacy was also obtained when the amide was converted to the thioamide. As evident from examples **6** and **8**, oral efficacy improved from 41% for the amide to 89% for the thio amide at 50 mg/kg/d. A similar but less dramatic effect was also observed with the 2-fluoro-4-bromo derivatives (examples **39** and **40**).

In conclusion, a novel series of (2-arylcarbamoyl-phenoxy)-acetic acid derivatives have been identified and optimized as highly potent and selective inhibitors of aldose reductase. In vivo evaluation of example **40**, 5-fluoro-2-(4-bromo-2-fluoro-benzylthiocarbamoyl)-phenoxyacetic acid, in the 4-day STZ-induced diabetic rat model resulted in lowered nerve sorbitol levels with an ED_{50} of 31 mg/kg/d (po). This compares favorably with tolrestat, an important aldose reductase inhibitor already developed for treatment of chronic diabetic complications. Continued development of these compounds may result in an important new treatment for chronic diabetic complications.

4. Experimental section

4.1. Chemistry

4.1.1. General methods. Melting points were determined in open capillary tubes on a Thomas–Hoover apparatus and are uncorrected. Proton nuclear magnetic resonance (^{1}H NMR) spectra were determined on a Varian Gemini 2000 (300 MHz) instrument. Chemical shifts are provided in parts per million (ppm) downfield from tetramethylsilane (internal standard) with coupling constants in hertz (Hz). Multiplicity is indicated by the following abbreviations: singlet (s), doublet (d), triplet (t), quartet (q), multiplet (m), broad (br). Mass spectra were recorded on a Perkin–Elmer API 100. Elemental analyses (C, H, N, S, Cl, Br) were performed by Atlantic Microlab, Inc. (Norcross, Georgia) and are within ±4% of theory unless otherwise noted. Products from all reactions were purified by either flash column chromatography or medium pressure liquid chromatography using silica gel 60 (230–400 mesh Kieselgel 60, EM Reagents) unless otherwise indicated. Thin-layer chromatography using glass-backed silica plates containing a fluorescent indicator (0.25 mm, Whatman, Merck) was used to monitor reactions. The chromatograms were visualized using ultraviolet illumination, exposure to iodine vapors, or dipped in an aqueous potassium permanganate solution. All starting materials were used without further purification. All reactions were carried out under an atmosphere of dried nitrogen.

4.1.2. General procedures for the synthesis of (2-arylcarbamoyl-phenoxy)-acetic acid derived ARIs. (2-Arylcarbamoyl-phenoxy)-acetic acids **6**, **8**, **13**, **34**–**56**, **61**–**4**, **66**, **69**, **72**–**74**, and **82**–**88** (Tables 1 and 2) were prepared from 2,4-difluorobenzoic acid **1** or the corresponding commercially available salicylic acids as outlined in Scheme 2 via the general experimental methods described, for examples, **6**, **8**, and **13** below. The substituted 2-aminothiophenol hydrochloride salts used to prepare examples **13** and **86**–**88** as illustrated were prepared by literature methods[32] or purchased commercially.

4.1.3. [5-Fluoro-2-(3-nitro-benzylcarbamoyl)-phenoxy]-acetic acid (6)

4.1.3.1. Step 1: synthesis of 4-fluoro-2-hydroxy-benzoic acid (2). A solution of 2,4-difluoro-benzoic acid (100 g, 0.63 mol) in 1,3-dimethyl-2-imidazolidinone (1400 mL, 0.45 M) was treated with sodium hydroxide (88 g, 2.2 mol) and heated to 135 °C. After stirring for 4 h, the solution was cooled to 0 °C and dissolved in water (100 mL). After transferring the solution to a 5 L Erlenmeyer flask, aq HCl (2800 mL, 2 N) was carefully added. After filtering off the crude product, the precipitate was dissolved in ethyl acetate, dried over sodium sulfate and decolorizing charcoal, and filtered. The solution was concentrated under reduced pressure and recrystallized from ethyl acetate and heptane to give 4-fluorosalicylic acid (two crops, 67 g, 68%) as off-white needles. Mp: 188–189 °C; R_f 0.26 (20% methanol in dichloromethane).

4.1.3.2. Step 2: synthesis of 4-fluoro-2-hydroxy-benzoyl chloride (3). A suspension of 4-fluoro-2-hydroxybenzoic acid (15 g, 96.1 mmol) in heptane (190 mL) was treated with thionyl chloride (21 mL, 288 mmol) in a dropwise manner over 30 min. A drop of *N*,*N*-dimethylformamide was added and the solution was heated for 4 h at 60 °C. The excess thionyl chloride was distilled off under reduced pressure. The remaining solution was cooled to room temperature, filtered, and concentrated to give 4-fluoro-2-hydroxy-benzoyl chloride as a pale yellow crystalline solid (14.2 g, 85%).

4.1.3.3. Step 3: synthesis of 4-fluoro-2-hydroxy-*N*-(3-nitro-benzyl)-benzamide (4). A solution of 4-fluoro-2-hydroxy-benzoyl chloride (12.3 g, 70.3 mmol) in dichloromethane (140 mL) was cooled to 0 °C, and treated with *N*,*N*-diisopropylethylamine (31.0 mL, 175 mmol) and 3-nitrobenzylamine hydrochloride (16 g, 84.6 mmol). After stirring at room temperature for 24 h, the solution was concentrated in vacuo and diluted with ethyl acetate. The organic layer was washed successively with aq 2 N HCl and saturated aq NaCl, dried over $MgSO_4$, filtered, and concentrated. Purification by MPLC (10–100% ethyl acetate in heptane, 23 mL/min, 75 min) provided

4-fluoro-2-hydroxy-*N*-(3-nitro-benzyl)-benzamide as a yellow solid (13.7 g, 67%): ^{1}H NMR (DMSO-d_6 300 MHz) δ 12.75 (s, 1H), 9.43 (t, J = 6.0 Hz, 1H), 8.11 (ddd, J_1 = 8.3 Hz, J_2 = 2.1 Hz, J_3 = 1.2 Hz, 1H), 8.18 (t, J = 1.5 Hz, 1H), 7.94 (dd, J_1 = 8.9 Hz, J_2 = 6.5 Hz, 1H), 7.78 (td, J_1 = 7.8 Hz, J_2 = 1.4 Hz, 1H), 7.63 (t, J = 8.0 Hz, 1H), 6.81–6.72 (m, 2H), 4.61 (d, J = 5.7 Hz, 2H).

4.1.3.4. Step 4: synthesis of [5-fluoro-2-(3-nitro-benzylcarbamoyl)-phenoxy]-acetic acid ethyl ester (5). A solution of 4-fluoro-2-hydroxy-*N*-(3-nitro-benzyl)-benzamide (5.00 g, 17.2 mmol) in acetone (86 mL) was treated with aq 2 N K_2CO_3 (13.0 mL, 25.8 mmol) and ethyl bromoacetate (1.50 mL, 9.66 mmol), and heated to 50 °C for 2 h. After cooling to 0 °C, the solution was acidified to pH 1 with 2 N HCl, diluted with ethyl acetate and washed with saturated aq NaCl. The organic layer was dried over $MgSO_4$, filtered, and concentrated. Purification by MPLC (10–100% ethyl acetate in heptane, 23 mL/min, 75 min) gave [5-fluoro-2-(3-nitro-benzylcarbamoyl)-phenoxy]-acetic acid ethyl ester as a pale yellow solid (6.1 g, 93%): mp 78–80 °C; R_f 0.26 (40% ethyl acetate in heptane); ^{1}H NMR (DMSO-d_6 300 MHz) δ 9.01 (t, J = 6.3 Hz, 1H), 8.19 (t, J = 1.8 Hz, 1H), 8.10 (dd, J_1 = 8.1 Hz, J_2 = 1.5 Hz, 1H), 7.89 (dd, J_1 = 8.7 Hz, J_2 = 6.9 Hz, 1H), 7.79 (d, J = 7.5 Hz, 1H), 7.61 (t, J = 8.1 Hz, 1H), 7.11 (dd, J_1 = 11.1 Hz, J_2 = 2.4 Hz, 1H), 6.92 (dt, J_1 = 8.4 Hz, J_2 = 2.4 Hz, 1H), 5.0 (s, 2H), 4.63 (d, J = 6.3 Hz, 2H), 4.15 (q, J = 7.2 Hz, 2H) 1.17 (t, J = 6.5 Hz, 3H). ESI-LC/MS *m/z* calcd for $C_{18}H_{17}FN_2O_6$: 376.4; found 377.0 $(M + 1)^+$. Anal. ($C_{18}H_{17}FN_2O_6$) C, H, N.

4.1.3.5. Step 5: synthesis of [5-fluoro-2-(3-nitro-benzylcarbamoyl)-phenoxy]-acetic acid (6). A suspension of [5-fluoro-2-(3-nitro-benzylcarbamoyl)-phenoxy]-acetic acid ethyl ester (3.3 g, 8.77 mmol) in ethanol (40 mL) was treated with aq 2 N NaOH (24 mL, 47.8 mmol). After stirring for 4 h, the solution was concentrated in vacuo until most of the ethanol was removed, and the mixture was acidified to pH 1 with 2 N HCl. After extracting with ethyl acetate, the organic layer was washed with saturated aq NaCl, dried over $MgSO_4$ and concentrated to give [5-fluoro-2-(3-nitro-benzylcarbamoyl)-phenoxy]-acetic acid as an off-white solid (3.00 g, 98%): mp 148–151 °C; R_f 0.39 (20% methanol in dichloromethane); ^{1}H NMR (DMSO-d_6 300 MHz) δ 9.20 (t, J = 6.3 Hz, 1H) 8.18 (s, 1H), 8.09 (dd, J_1 = 7.2 Hz, J_2 = 2.7 Hz, 1H), 7.90 (dd, J_1 = 8.7 Hz, J_2 = 7.0 Hz, 1H), 7.79 (d, J = 7.5 Hz, 1H), 7.61 (t, J = 7.8 Hz, 1H), 7.08 (dd, J_1 = 10.8 Hz, J_2 = 2.1 Hz, 1H), 6.91 (dt, J_1 = 8.7 Hz, J_2 = 2.4 Hz, 1H), 4.89 (s, 2H), 4.62 (d, J = 6.3 Hz, 2H). ESI-LC/MS *m/z* calcd for $C_{16}H_{13}FN_2O_6$: 348.3; found 347.0 $(M-1)^-$. Anal. ($C_{16}H_{13}FN_2O_6$) C, H, N.

4.1.4. [5-Fluoro-2-(3-nitro-benzylthiocarbamoyl)-phenoxy]-acetic acid (8)

4.1.4.1. Step 1: synthesis of [5-fluoro-2-(3-nitro-benzylthiocarbamoyl)-phenoxy]-acetic acid ethyl ester (7). In a flame dried flask under a nitrogen atmosphere, a suspension of phosphorous pentasulfide (0.77 g, 1.73 mmol) in pyridine (6.9 mL) was treated with [5-fluoro-2-(3-nitro-benzylcarbamoyl)-phenoxy]-acetic acid ethyl ester (example 6, 1.3 g, 3.45 mmol) and heated to 115 °C for 4 h. After cooling to room temperature, the mixture was diluted with water and ethyl acetate. The organic layer was washed successively with 2 N HCl and saturated NaCl, dried over $MgSO_4$, and concentrated. The resulting dark orange solid was filtered through a short pad of silica with ethyl acetate and concentrated to give [5-fluoro-2-(3-nitro-benzylthiocarbamoyl)-phenoxy]-acetic acid ethyl ester as an orange solid (1.2 g, 89%): mp 118 °C; R_f 0.43 (40% ethyl acetate in heptane); ^{1}H NMR (DMSO-d_6 300 MHz) δ 10.71 (br s, 1H), 8.23 (s, 1H), 8.12 (d, J = 8.1 Hz, 1H), 7.83 (d, J = 7.8 Hz, 1H), 7.71–7.60 (m, 2H), 7.04 (dd, J_1 = 11.1 Hz, J_2 = 2.4 Hz, 1H), 6.87 (dt, J_1 = 8.4 Hz, J_2 = 2.4 Hz, 1H), 5.07 (d, J = 3.3 Hz, 2H), 4.89 (s, 2H), 4.13 (q, J = 6.7 Hz, 2H), 1.17 (t, J = 5.7 Hz, 3H). ESI-LC/MS *m/z* calcd for $C_{18}H_{17}FN_2O_5S$: 394.1; found 393.0 $(M + 1)^+$. Anal. ($C_{18}H_{17}FN_2O_5S$) C, H, N.

4.1.4.2. Step 2: [5-Fluoro-2-(3-nitro-benzylthiocarbamoyl)-phenoxy]-acetic acid (8). A suspension of [5-fluoro-2-(3-nitro-benzylthiocarbamoyl)-phenoxy]-acetic acid ethyl ester (4.39 g, 11.2 mmol) in ethanol (40 mL) was treated with aq 2 N NaOH (11 mL, 22.4 mmol). After stirring for 4 h, the solution was concentrated under reduced pressure until most of the ethanol was removed, and the mixture was acidified to pH 1 with 2 N HCl. After extracting with ethyl acetate, the organic layer was washed with saturated aq NaCl, dried over $MgSO_4$, and concentrated to give [5-fluoro-2-(3-nitro-benzylthiocarbamoyl)-phenoxy]-acetic acid (4.0 g, 98%) as an off-white solid: mp 147–150 °C; R_f 0.27 (20% methanol in dichloromethane); ^{1}H NMR (DMSO-d_6 300 MHz) δ 13.23 (s, 1H), 10.79 (t, J = 5.7 Hz, 1H), 8.23 (t, J = 1.8 Hz, 1H), 8.11 (ddd, J_1 = 8.3 Hz, J_2 = 2.7 Hz, J_3 = 1.2 Hz, 1H), 7.85 (br d, J = 7.5 Hz, 1H), 7.73 (dd, J_1 = 8.9 Hz, J_2 = 7.1 Hz, 1H), 7.63 (t, J = 8.1 Hz, 1H), 7.03 (dd, J_1 = 11.4 Hz, J_2 = 2.4 Hz, 1H), 6.86 (dt, J_1 = 8.4 Hz, J_2 = 2.4 Hz, 1H), 5.07 (d, J = 5.7 Hz, 2H), 4.83 (s, 2H). ESI-LC/MS *m/z* calcd for $C_{16}H_{13}FN_2O_5S$: 364.4; found 363.0 $(M-1)^-$. Anal. ($C_{16}H_{13}FN_2O_5S$) C, H, N.

4.1.5. {5-Fluoro-2[(4,5,7-trifluoro-benzothiazol-2-ylmethyl)carbamoyl]-phenoxy}-acetic acid (13)

4.1.5.1. Step 1: synthesis of *N*-cyanomethyl-4-fluoro-2-hydroxy-benzamide (9). A solution of 4-fluorosalicylic acid chloride (example 6, 10 g, 57.3 mmol) in dichloromethane (114 mL) was treated with *N*,*N*-diisopropyl-ethyl amine (25 mL, 143 mmol) and acetonitrile hydrochloride (7.95 g, 85.9 mmol). After stirring at 35 °C for 24 h, the solution was concentrated under reduced pressure, diluted with ethyl acetate, and washed successively with 2 N HCl and saturated aq NaCl. The resulting solution was dried over $MgSO_4$, filtered, and concentrated. The resulting solid was suspended in dichloromethane, filtered, and rinsed with heptane to give *N*-cyanomethyl-4-fluoro-2-hydroxy-benzamide as

a pale yellow solid (7.20 g, 65%): ^{1}H NMR (DMSO-d_6 300 MHz) δ 12.16 (br s, 1H), 9.17 (t, J = 5.3 Hz, 1H), 7.88 (dd, J_1 = 8.7 Hz, J_2 = 6.3 Hz, 1H), 6.81–6.73 (m, 2H), 4.32 (d, J = 5.7 Hz, 2H).

4.1.5.2. Step 2: synthesis of 4-fluoro-2-hydroxy-*N*-(4,5,7,-trifluoro-benzothiazol-2-ylmethyl)-benzamide (11). A solution of *N*-cyanomethyl-4-fluoro-2-hydroxy-benzamide (2.93 g, 13.6 mmol) and 2-amino-4,5,7-trifluorothiophenol hydrochloride[33,34] (6.64 g, 13.6 mmol) in ethanol (27.2 mL) was heated to reflux for 24 h. After cooling to room temperature, the mixture was concentrated in vacuo, diluted with water and extracted with ethyl acetate. The organic layer was washed with saturated aq NaCl, dried over $MgSO_4$, filtered, and concentrated. Purification by MPLC (10–100% ethyl acetate in heptane, 23 mL/min, 75 min) provided 4-fluoro-2-hydroxy-*N*-(4,5,7,-trifluoro-benzothiazol-2-ylmethyl)-benzamide (1.00 g, 21%) as a white crystalline solid: ^{1}H NMR (DMSO-d_6 300 MHz) δ 12.35 (br s, 1H), 9.70 (t, J = 5.4 Hz, 1H), 7.95 (dd, J_1 = 8.9 Hz, J_2 = 6.8 Hz, 1H), 7.80–7.70 (m, 1H), 6.83–6.74 (m, 2H), 4.94 (t, J = 3 Hz, 2H).

4.1.5.3. Step 3: synthesis of {5-fluoro-2[(4,5,7-trifluoro-benzothiazol-2-ylmethyl)carbamoyl]-phenoxy}-acetic acid ethyl ester (12). A solution of 4-fluoro-2-hydroxy-*N*-(4,5,7,-trifluoro-benzothiazol-2-ylmethyl)-benzamide (1.0 g, 2.8 mmol) in acetone (14 mL) was treated with aq 2 N K_2CO_3 (2.1 mL, 4.2 mmol) and ethyl bromoacetate (2 mL, 19 mmol) and heated to 45 °C for 5 h. After cooling to room temperature, the solution was acidified to a pH 1 with aq 2 N HCl. The resulting solution was diluted with ethyl acetate and washed with saturated NaCl. The organic layer was dried over $MgSO_4$, filtered, and concentrated. Purification by MPLC (10–100% ethyl acetate in heptane 23 mL/min, 75 min) provided {5-fluoro-2[(4,5,7-trifluoro-benzothiazol-2-ylmethyl)carbamoyl]-phenoxy}-acetic acid ethyl ester (1.0 g, 81%) as a white crystalline solid: ^{1}H NMR (DMSO-d_6 300 MHz) δ 9.32 (t, J = 5.9 Hz, 1H), 7.94 (dd, J_1 = 9.0 Hz, J_2 = 7.2 Hz, 1H), 7.80–7.70 (m, 1H), 7.13 (dd, J_1 = 11.1 Hz, J_2 = 2.4 Hz, 1H), 6.95 (dt, J_1 = 8.4 Hz, J_2 = 2.5 Hz, 1H), 5.02 (s, 2H), 4.94 (d, J = 6 Hz, 2H), 4.17 (q, J = 7.2 Hz, 2H), 1.18 (t, J = 7.1 Hz, 3H).

4.1.5.4. Step 4: synthesis of {5-fluoro-2[(4,5,7-trifluoro-benzothiazol-2-ylmethyl)carbamoyl]-phenoxy}-acetic acid (13). A suspension of {5-fluoro-2[(4,5,7-trifluoro-benzothiazol-2-ylmethyl)carbamoyl]-phenoxy}-acetic acid ethyl ester (1 g, 2.3 mmol) in ethanol (11 mL) was treated with aq 2 N NaOH (6.8 mL, 14 mmol) and stirred at room temperature. After 1 h, the solution was concentrated in vacuo and acidified to pH 1 with aq 2 N HCl. The resulting solution was diluted with ethyl acetate and washed with saturated NaCl. The organic layer was dried over $MgSO_4$, filtered, and concentrated to give {5-fluoro-2[(4,5,7-trifluoro-benzothiazol-2-ylmethyl)carbamoyl]-phenoxy}-acetic acid. (0.68 g, 73%) as a white crystalline solid. Mp 172–174 °C; R_f 0.38 (20% methanol in dichloromethane); ^{1}H NMR (DMSO-d_6 300 MHz) δ 13.25 (br s, 1H), 9.49 (t, J = 6 Hz, 1H), 7.95 (dd, J_1 = 9 Hz, J_2 = 7.2 Hz, 1H), 7.78–7.69 (m, 1H), 7.11 (dd, J_1 = 11.0 Hz, J_2 = 2.3 Hz, 1H), 6.94 (dd, J_1 = 8.4 Hz, J_2 = 2.4 Hz, 1H), 4.94–4.92 (m, 4H). ESI-LC/MS *m/z* calcd for $C_{17}H_{10}F_4N_2O_4S$: 414.3; found 413.0 $(M-1)^-$. Anal. ($C_{17}H_{10}F_4N_2O_4S$) C, H, N.

The 2-fluoro-3-methyl examples **24**, **25**, **80**, and **81** were prepared from 5-methoxy-2-methyl-4-nitro-phenylamine as illustrated in Scheme 3 and described in detail below.

4.1.6. [2-(4-Bromo-2-fluoro-benzylcarbamoyl)-5-fluoro-4-methyl-phenoxy]-acetic acid (25)

4.1.6.1. Step 1: synthesis of 1-fluoro-5-methoxy-2-methyl-4-nitro-benzene (15). Under an atmosphere of nitrogen in a Nalgene bottle, a stirring solution of pyridine (17.1 mL, 3.2 M, −70 °C) was treated dropwise with HF-pyridine (51.91 mL). 5-Methoxy-2-methyl-4-nitro-phenylamine (10.0 g, 54.9 mmol) was added and the mixture was treated with sodium nitrite (6.4 g, 92.76 mmol). The reaction was allowed to warm to room temperature over 45 min and subsequently heated to 60 °C for 2 h (until nitrogen evolution stops). After cooling to room temperature, the Nalgene bottle was placed in an ice bath and 375 mL of water was slowly added to the solution. The resulting orange precipitate was collected by suction filtration and washed with 250 mL of water. Purification of the solid via silica gel flash chromatography (30% ethyl acetate in heptane) provided 1-fluoro-5-methoxy-2-methyl-4-nitro-benzene (7.69 g, 76%) as a light orange solid: mp 71–74 °C; R_f 0.56 (30% ethyl acetate in heptane); ^{1}H NMR ($CDCl_3$, 300 MHz) δ 7.82 (d, J = 7.5 Hz, 1H), 6.75 (d, J = 10.5 Hz, 1H), 3.93 (s, 3H), 2.25 (d, J = 2.1 Hz, 3H); ESI-LC/MS *m/z* calcd for $C_8H_8FNO_3$: 185.1; found 186.0 $(M+1)^+$. Anal. ($C_8H_8FNO_3$) C, H, N.

4.1.6.2. Step 2: synthesis of 4-fluoro-2-methoxy-5-methyl-phenylamine (16). A solution of 1-fluoro-5-methoxy-2-methyl-4-nitro-benzene (5.5 g, 29.3 mmol) and 10% Pd–C (1.56 g) in ethanol (300 mL, 0.1 M) was hydrogenated at 1 atm. After stirring overnight, the solution was flushed through a pad of silica gel using 400 mL of ethanol as the eluant. The filtrate was concentrated under reduced pressure to afford 4-fluoro-2-methoxy-5-methyl-phenylamine (4.5 g, 99%) as a pale purple solid: mp 108–110 °C; R_f 0.35 (30% ethyl acetate in heptane); ^{1}H NMR (DMSO-d_6, 300 MHz) δ 6.62 (d, J = 11.4 Hz, 1H), 6.43 (d, J = 7.8 Hz, 1H), 3.70 (s, 3H), 2.02 (d, J = 1.8 Hz, 3H); ESI-LC/MS *m/z* calcd for $C_8H_{10}FNO$: 155.1; found 156.0 $(M+1)^+$. Anal. ($C_8H_{10}FNO$) C, H, N.

4.1.6.3. Step 3: synthesis of 1-bromo-4-fluoro-2-methoxy-5-methyl-benzene (17). A suspension of 4-fluoro-2-methoxy-5-methyl-phenylamine (25.75 g, 0.17 mol) in 180 mL of HBr (48%, 0.9 M) in an ice bath was carefully treated with an aq solution of sodium nitrite (12.6 g, 0.18 mol, 3.6 M). Throughout the addition, a brown gas was evolved and the temperature of the reaction was monitored so that the internal temperature did not raise above 10 °C. In parallel, a suspension of CuBr

(13.1 g, 0.09 mol) in 6.5 mL of HBr (48%, 13.9 M) was heated to 110 °C and carefully treated with the first solution (over 20 min). The combined reaction mixture was heated for 2.5 h at 110 °C, cooled to room temperature, diluted with ethyl acetate, and treated with aq sulfuric acid (50% v/v). The organic layer was separated and washed successively with water, sulfuric acid (50% v/v), water, 1.25 M NaOH, water, and saturated aq NaCl. The organic layer was dried over Na_2SO_4, filtered, and concentrated under reduced pressure. Purification of the resulting brown oil via silica gel flash chromatography (5% ethyl acetate in heptane) provided 1-bromo-4-fluoro-2-methoxy-5-methyl-benzene (17.1 g, 47%) as a colorless liquid: R_f 0.70 (30% ethyl acetate in heptane); ^{1}H NMR ($CDCl_3$, 300 MHz) δ 7.34 (d, $J = 8.4$ Hz, 1H), 6.61 (d, $J = 10.8$ Hz, 1H), 3.85 (s, 3H), 2.18 (d, $J = 1.8$ Hz, 3H); Anal. (C_8H_8BrFO) C, H, Br.

4.1.6.4. Step 4: synthesis of 4-fluoro-2-methoxy-5-methyl-benzonitrile (18). A solution of 1-bromo-4-fluoro-2-methoxy-5-methyl-benzene (5.0 g, 22.8 mmol) in DMF (100 mL, 0.2 M) was treated with CuCN (4.7 g, 52.5 mmol) and heated to 160 °C for 20 h. After cooling to room temperature, the solution was poured into a 2 L Erlenmeyer flask. Ethyl acetate (400 mL), saturated aq LiCl (100 mL), 1 N HCl (100 mL), iron(III) chloride hexahydrate (11 g), and 15 mL of concd HCl were added to the solution. The resulting green mixture was heated at 70 °C for 2 h (until emulsion dissipated). After cooling to room temperature, the mixture was poured into a separatory funnel and extracted with ethyl acetate (3×200 mL). The combined organic extracts were washed successively with 1 N HCl (200 mL), saturated aq LiCl (2×200 mL), and saturated aq NaCl (100 mL). The organic layer was dried over Na_2SO_4, filtered, and concentrated under reduced pressure. The resulting powder was dissolved in ethyl acetate (50 mL) and washed with saturated aq LiCl (3×30 mL), dried over Na_2SO_4, filtered, and concentrated under reduced pressure to afford 4-fluoro-2-methoxy-5-methyl-benzonitrile (3.25 g, 86%) as an off-white powder: mp 99–101 °C; R_f 0.53 (30% ethyl acetate in heptane); ^{1}H NMR ($CDCl_3$, 300 MHz) δ 7.39 (d, $J = 8.1$ Hz, 1H), 6.65 (d, $J = 11.1$ Hz, 1H), 3.89 (d, $J = 0.9$ Hz, 3H), 2.21 (s, 3H). Anal. (C_9H_8FNO) C, H, N.

4.1.6.5. Step 5: synthesis of 4-fluoro-2-methoxy-5-methyl-benzoic acid (19). A suspension of 4-fluoro-2-methoxy-5-methyl-benzonitrile (3.0 g, 18.2 mmol) in 2 N NaOH (300 mL, 0.06 M) was heated to 90 °C for 19 h. The remaining starting material was recovered by filtration (0.86 g). The aqueous solution was acidified to pH 1 (concentrated HCl) and extracted with ethyl acetate (2×250 mL). The combined organic extracts were dried over Na_2SO_4, filtered, and concentrated to afford 4-fluoro-2-methoxy-5-methyl-benzoic acid as a white powder (2.28 g, 96% based on recovered starting material): mp 125–127 °C; R_f 0.15 (40% ethyl acetate in heptane); ^{1}H NMR ($CDCl_3$, 300 MHz) δ 10.20 (s, 1H), 8.05 (d, $J = 9.0$ Hz, 1H), 6.74 (d, $J = 10.8$ Hz, 1H), 4.04 (s, 3H), 2.25 (d, $J = 1.8$ Hz, 3H); ESI-LC/MS *m/z* calcd for $C_9H_9FO_3$: 184.1; found 185.0 $(M + 1)^+$. Anal. ($C_9H_9F0_3$) C, H, N.

4.1.6.6. Step 6: synthesis of *N*-(4-bromo-2-fluoro-benzyl)-4-fluoro-2-methoxy-5-methyl-benzamide (20). Under a nitrogen atmosphere, a solution of 4-fluoro-2-methoxy-5-methyl-benzoic acid (1.19 g, 6.47 mmol) in dichloromethane (16 mL, 0.5 M) was treated with oxalyl chloride (1.7 mL, 19.4 mmol) and a drop of DMF at 0 °C. The mixture was allowed to gradually warm to room temperature over 30 min and subsequently concentrated. The resulting yellow powder was dissolved in dichloromethane (16 mL, 0.5 M), cooled to 0 °C and treated with diisopropylethylamine (2.8 mL, 16.2 mmol) and 4-bromo-2-fluorobenzylamine hydrochloride salt (2.34 g, 9.71 mmol). The mixture was warmed to room temperature and stirred for 21 h. The resulting solution was washed successively with 1 N HCl (3×50 mL) and saturated aq NaCl (50 mL). The organic layer was dried over Na_2SO_4, filtered, and concentrated to afford *N*-(4-bromo-2-fluoro-benzyl)-4-fluoro-2-methoxy-5-methyl-benzamide (2.33 g, 97%) as a brown oil, which was used without further purification: R_f 0.40 (30% ethyl acetate in heptane); ^{1}H NMR ($CDCl_3$, 300 MHz) δ 8.17 (br s, 1H), 8.06 (d, $J = 9.3$ Hz, 1H), 7.33–7.22 (m, 3H), 6.65 (d, $J = 11.1$ Hz, 1H), 4.63 (d, $J = 6.3$ Hz, 2H), 3.92 (s, 3H), 2.23 (br d, $J = 1.8$ Hz, 3H).

4.1.6.7. Step 7: synthesis of *N*-(4-bromo-2-fluoro-benzyl)-4-fluoro-2-hydroxy-5-methyl-benzamide (21). A stirring suspension of *N*-(4-bromo-2-fluoro-benzyl)4-fluoro-2-methoxy-5-methyl-benzamide (2.32 g, 6.51 mmol) in a 25% solution of HBr in acetic acid (60 mL, 0.11 M) was heated to 120 °C for 3.5 h. After cooling to room temperature, saturated aq NaCl (50 mL) was added and the solution was extracted with ethyl acetate (3×50 mL). The combined organic extracts were dried over Na_2SO_4, filtered, and concentrated. The resulting orange powder was purified via silica gel flash chromatography (30% ethyl acetate in heptane) to give *N*-(4-bromo-2-fluoro-benzyl)-4-fluoro-2-hydroxy-5-methyl-benzamide (1.69, 73%) as a white powder: mp 149–150 °C; R_f 0.51 (30% ethyl acetate in heptane); ^{1}H NMR ($CDCl_3$, 300 MHz) δ 12.20 (d, $J = 1.5$ Hz, 1H), 7.30–7.29 (m, 2H), 7.26 (s, 1H), 7.14 (d, $J = 8.1$ Hz, 1H), 6.64 (d, $J = 10.8$ Hz, 1H), 6.48 (br s, 1H), 4.62 (d, $J = 5.7$ Hz, 2H), 2.19 (s, 3H); ESI-LC/MS *m/z* calcd for $C_{15}H_{12}BrF_2NO_2$: 355.0; found 354.0 $(M-1)^-$. Anal. ($C_{15}H_{12}BrF_2NO_2$) C, H, N.

4.1.6.8. Step 8: synthesis of [2-(4-bromo-2-fluoro-benzylcarbamoyl)-5-fluoro-4-methyl-phenoxy]-acetic acid ethyl ester (22). A stirring solution of *N*-(4-bromo-2-fluoro-benzyl)-4-fluoro-2-hydroxy-5-methyl-benzamide (1.69 g, 4.76 mmol) in acetone (24 mL, 0.2 M) was treated with a second solution of aq K_2CO_3 (3.6 mL, 2 M, 7.12 mmol) and ethyl bromoacetate (0.63 mL, 5.69 mmol) in acetone (24 mL, 0.2 M). After heating to 50 °C for 2.5 h, the solution was cooled to room temperature, concentrated, and acidified to pH 1 with 2 N HCl. The resulting solution was diluted with ethyl acetate (100 mL) and washed with saturated aq NaCl (50 mL). The organic layer was dried over Na_2SO_4, filtered, and concentrated to provide [2-(4-bromo-2-fluoro-benzylcarbamoyl)-5-fluoro-4-methyl-phenoxy]-acetic acid ethyl ester (1.95, 93%) as a white solid: mp 128–129 °C; R_f

0.42 (30% ethyl acetate in heptane); ^{1}H NMR ($CDCl_3$, 300 MHz) δ 8.79 (br t, J = 4.5 Hz, 1H), 8.10 (d, J = 9.0 Hz, 1H), 7.34 (t, J = 8.3 Hz, 1H), 7.26–7.23 (m, 1H), 7.21 (t, J = 2.3 Hz, 1H), 6.53 (d, J = 10.5 Hz, 1H), 4.66 (d, J = 3.9 Hz, 1H), 4.65 (s, 2H), 4.28 (q, J = 7.2 Hz, 2H), 2.23 (br d, J = 1.5 Hz, 3H), 1.30 (t, J = 7.2 Hz, 3H); Anal. ($C_{19}H_{18}BrF_2NO_4$) C, H, N.

4.1.6.9. Step 9: synthesis of [2-(4-bromo-2-fluoro-benzylcarbamoyl)-5-fluoro-4-methyl-phenoxy]-acetic acid (25). A solution of [2-(4-bromo-2-fluoro-benzylcarbamoyl)-5-fluoro-4-methyl-phenoxy]-acetic acid ethyl ester (0.72 g, 1.62 mmol) in ethanol (8.1 mL, 0.2 M) was cooled to 0 °C and treated with aq NaOH (1.25 M, 7.8 mL, 9.73 mmol). After the addition was complete, the mixture was warmed to room temperature and stirred an additional 2 h. The resulting solution was concentrated under reduced pressure, acidified with 2 N HCl (10 mL) and diluted with ethyl acetate. The separated organic layer was washed with saturated aq NaCl, dried over Na_2SO_4, filtered, and concentrated to afford [2-(4-bromo-2-fluoro-benzylcarbamoyl)-5-fluoro-4-methyl-phenoxy]-acetic acid (0.66 g, 98%) as a white solid: mp 169 °C; R_f 0.22 (20% methanol in dichloromethane); ^{1}H NMR (DMSO-d_6, 300 MHz) δ 9.00 (br t, J = 5.3 Hz, 1H), 7.76 (d, J = 9.6 Hz, 1H), 7.49 (d, J = 9.6 Hz, 1H), 7.39–7.33 (m, 2H), 7.04 (dd, J_1 = 11.4 Hz, J_2 = 1.4 Hz, 1H), 4.84 (d, J = 1.8 Hz, 2H), 4.48 (br s, 2H), 2.17 (s, 3H); ESI-LC/MS m/z calcd for $C_{17}H_{14}BrF_2NO_4$: 413.0; found 412.0 $(M-1)^-$. Anal. ($C_{17}H_{14}BrF_2NO_4$) C, H, N.

4.1.7. [2-(4-Bromo-2-fluoro-benzylthiocarbamoyl)-5-fluoro-4-methyl-phenoxy]-acetic acid (24)

4.1.7.1. Step 1: synthesis of [2-(4-bromo-2-fluoro-benzylthiocarbamoyl)-5-fluoro-4-methyl-phenoxy]-acetic acid ethyl ester (23). A solution of [2-(4-bromo-2-fluoro-benzylcarbamoyl)-5-fluoro-4-methyl-phenoxy]-acetic acid ethyl ester (example **25**, 0.816 g, 1.83 mmol) in pyridine (3.7 mL, 0.5 M) was treated with phosphorous pentasulfide (0.41 g, 0.92 mmol) and heated to 115 °C for 3 h. The reaction was cooled to room temperature, diluted with ethyl acetate and successively washed with 1 M HCl and saturated aq NaCl. The organic layer was dried over Na_2SO_4, filtered, and concentrated under reduced pressure. The resulting brown oil was dissolved in a minimal amount of methylene chloride and flushed through a plug of silica using 40% ethyl acetate in heptane as the eluant. The filtrate was concentrated to afford [2-(4-bromo-2-fluoro-benzylthiocarbamoyl)-5-fluoro-4-methyl-phenoxy]-acetic acid ethyl ester (0.75 g, 89%) as a yellow solid: mp 98–100 °C; R_f 0.45 (30% ethyl acetate in heptane); ^{1}H NMR ($CDCl_3$, 300 MHz) δ 10.15 (br s, 1H), 8.26 (d, J = 8.4 Hz, 1H), 7.38 (t, J = 8.4 Hz, 1H), 7.26–7.23 (m, 2H), 6.53 (d, J = 10.8 Hz, 1H), 5.08 (d, J = 5.4 Hz, 2H), 4.67 (s, 2H), 4.20 (q, J = 7.2 Hz, 2H), 2.23 (s, 3H), 1.27 (t, J = 6.8 Hz, 3H).

4.1.7.2. Step 2: synthesis of [2-(4-bromo-2-fluoro-benzylthiocarbamoyl)-5-fluoro-4-methyl-phenoxy]-acetic acid (24). A solution of [2-(4-bromo-2-fluoro-benzylthiocarbamoyl)-5-fluoro-4-methyl-phenoxy]-acetic acid ethyl ester (0.79 g, 1.53 mmol) in ethanol (7.6 mL, 0.2 M) was treated with aqueous NaOH (2 N, 7.4 mL, 9.15 mmol). After stirring for 4 h, the solution was concentrated under reduced pressure until most of the ethanol was removed. The remaining solution was acidified to pH 1 with 2 N HCl and extracted with ethyl acetate. The organic layer was washed with saturated aq NaCl, dried over $MgSO_4$ and concentrated to give [2-(4-bromo-2-fluoro-benzylthiocarbamoyl)-5-fluoro-4-methyl-phenoxy]-acetic acid (0.65 g, 98%) as a yellow solid: mp 162–164 °C; R_f 0.41 (20% methanol in dichloromethane); ^{1}H NMR (DMSO-d_6, 300 MHz) δ 10.64 (t, J = 5.0 Hz, 1H), 7.61 (d, J = 9.0 Hz, 1H), 7.52 (dd, J_1 = 9.6 Hz, J_2 = 1.7 Hz, 1H), 7.45–7.36 (m, 2H), 7.00 (d, J = 11.4 Hz, 1H), 4.89 (br d, J = 5.1 Hz, 2H), 4.78 (s, 2H), 2.15 (d, J = 1.2 Hz, 3H); ESI-LC/MS m/z calcd for $C_{17}H_{14}BrF_2NO_3S$: 428.98; found 428.0 $(M-1)^-$; Anal. ($C_{17}H_{14}BrF_2NO_3S$) C, H, N, S.

Examples **75**–**79** were prepared from salicylic acid derivatives **26**, **29**, **31**, and **33** using the general method described, for examples, **24** and **25**. Salicylic acid derivatives **26**, **29**, **31**, and **33** were prepared using the method illustrated in Scheme 4 and described in detail below.

4.1.8. 5-Bromo-4-fluoro-2-hydroxy-benzoic acid (26). A solution of 4-fluoro-2-hydroxy-benzoic acid (5.58 g, 35.7 mmol) in dimethylformamide (72 mL, 0.5 M) was treated with *N*-bromosuccinimide (7.08 g, 39.3 mmol) and stirred for 24 h at room temperature. The resulting mixture was diluted with ethyl acetate (300 mL) and washed successively with water (3 × 330 mL) and saturated aq LiCl (4 × 200 mL). The combined organic layers were dried over Na_2SO_4, filtered, and concentrated to give 5-bromo-4-fluoro-2-hydroxy-benzoic acid (8.1 g, 96%) as an off-white powder. R_f 0.32 (20% methanol in dichloromethane); ^{1}H NMR (DMSO-d_6, 300 MHz) δ 8.00 (d, J = 8.1 Hz, 1H), 7.05 (d, J = 10.5 Hz, 1H).

4.1.9. 5-Bromo-4-fluoro-2-methoxy-benzoic acid methyl ester (27). A solution of 5-bromo-4-fluoro-2-hydroxy-benzoic acid (15.0 g, 63.8 mmol) and anhydrous K_2CO_3 (19 g, 140 mmol) in acetone (128 mL, 0.5 M) was treated with iodomethane (24 mL, 380 mmol) and heated to 60 °C for 4 h. After cooling to room temperature, the solution was concentrated and purified by MPLC (10–100% ethyl acetate in heptane, 23 mL/min, 70 min) to give 5-bromo-4-fluoro-2-methoxy-benzoic acid methyl ester (13.52 g, 80%) as a white solid: mp 73–77 °C; R_f 0.56 (40% ethyl acetate in heptane); ^{1}H NMR ($CDCl_3$, 300 MHz) δ 8.05 (d, J = 7.8 Hz, 1H), 6.76 (d, J = 10.5 Hz, 1H), 3.89 (s, 3H), 3.88 (s, 3H). Anal. ($C_9H_6BrFO_3$) C, H, Br.

4.1.10. 4-Fluoro-2-methoxy-5-morpholin-4-yl-benzoic acid methyl ester (28). A solution of oven-dried cesium carbonate (4.33 g, 13.3 mmol), palladium acetate (85.3 mg, 0.380 mmol), R-(+)-2,2′-bis(diphenylphosphino)-1,1′-binaphthyl (0.355 g, 0.570 mmol) and 5-bromo-4-fluoro-2-methoxy-benzoic acid methyl ester

(2.50 g, 9.50 mmol) in toluene (0.76 mL) was treated with morpholine (0.99 mL, 11.4 mmol) and heated to 100 °C for 24 h. After cooling to room temperature the solution was diluted with ether, filtered, and concentrated. Purification by MPLC (10–50% ethyl acetate in heptane, 23 mL/min, 35 min) provided 4-fluoro-2-methoxy-5-morpholin-4-yl-benzoic acid methyl ester (1.20 g, 47%): ^{1}H NMR (DMSO-d_6 300 MHz) δ 7.33 (d, J = 9.9 Hz, 1H), 7.08 (d, J = 14.4 Hz, 1H), 3.76 (s, 3H), 3.75 (s, 3H), 3.70 (t, J = 4.7 Hz, 4H), 2.90 (t, J = 4.5 Hz, 4H).

4.1.11. 4-Fluoro-2-methoxy-5-morpholin-4-yl-benzoic acid (29). A suspension of 4-fluoro-2-methoxy-5-morpholin-4-yl-benzoic acid methyl ester (1.20 g, 4.46 mmol) in ethanol (22.0 mL) was treated with aq 2 N NaOH (13 mL, 26.7 mmol) and stirred at room temperature for 2 h. The resulting solution was concentrated until most of the ethanol was removed and subsequently acidified to pH 1 with aq 2 N HCl. After extracting with ethyl acetate, the organic layer was washed with saturated aq NaCl, dried over $MgSO_4$ and concentrated to give 4-fluoro-2-methoxy-5-morpholin-4-yl-benzoic acid as a pale yellow foam (0.90 g, 79%): ^{1}H NMR (DMSO-d_6 300 MHz) δ 12.62 (s, 1H), 7.34 (d, J = 10.5 Hz, 1H), 7.04 (d, J = 14.7 Hz, 1H), 3.76 (s, 3H), 3.70 (t, J = 4.7 Hz, 4H), 2.90 (t, J = 4.7 Hz, 4H).

4.1.12. 5-Cyano-4-fluoro-2-methoxy-benzoic acid methyl ester (30). A solution of 5-bromo-4-fluoro-2-methoxy-benzoic acid methyl ester (5.0 g, 10.0 mmol) in DMF (38 mL, 0.5 M) was treated with CuCN (3.92 g, 43.7 mmol) and heated at 150 °C for 24 h. After cooling to room temperature, the solution was transferred to an Erlenmeyer flask and diluted with ethyl acetate (400 mL), saturated aq LiCl (100 mL), 1 N HCl (100 mL), 11 g of iron(III) chloride hexahydrate, and 15 mL of concd HCl. The resulting green mixture was heated to 70 °C until the emulsion dissipated (2 h). After cooling to room temperature, the mixture was extracted with ethyl acetate (600 mL) and successively washed with 1 N HCl (200 mL), saturated aq LiCl (2 × 200 mL) and saturated aq NaCl (100 mL). The organic layer was dried over Na_2SO_4, filtered, and concentrated under reduced pressure. Purification by MPLC (10–100% ethyl acetate in heptane, 23 mL/min, 75 min) provided 5-cyano-4-fluoro-2-methoxy-benzoic acid methyl ester (2.98 g, 75%) as a white crystalline solid: ^{1}H NMR ($CDCl_3$, 300 MHz) δ 8.15 (d, J = 7.5 Hz, 1H), 6.80 (d, J = 11.1 Hz, 1H), 3.97 (s, 3H), 3.90 (s, 3H).

4.1.13. 5-Cyano-4-fluoro-2-methoxy-benzoic acid (31). A stirring suspension of 5-cyano-4-fluoro-2-methoxy-benzoic acid methyl ester (2.98 g, 14.25 mmol) in ethanol (30 mL, 0.5 M) was treated with 1.25 M NaOH (68 mL, 85.5 mmol) and stirred for 10 min (solution becomes clear). The reaction mixture was concentrated to about 10% of its original volume and acidified to pH 1 with 2 N HCl. The resulting white precipitate was collected by suction filtration, dissolved in dioxane, and washed with aq saturated NaCl. The organic layer was dried over Na_2SO_4, filtered, and concentrated to afford 5-cyano-4-fluoro-2-methoxy-benzoic acid (1.9 g, 70%) as a white solid. R_f = 0.34 (20% methanol in dichloromethane); ^{1}H NMR ($CDCl_3$, 300 MHz) δ 8.13 (d, J = 8.1 Hz, 1H), 7.36 (d, J = 12.0 Hz, 1H), 3.90 (s, 3H).

4.1.14. 6-Fluoro-4-methoxy-biphenyl-3-carboxylic acid methyl ester (32). A solution of 5-bromo-4-fluoro-2-methoxy-benzoic acid methyl ester (2.0 g, 7.6 mmol), anhydrous K_2CO_3 (2.1 g, 15 mmol), and phenylboronic acid (3.7 g, 30.4 mmol) in degassed toluene (15.2 mL, 0.5 M) was treated with $Pd(PPh_3)_4$ (0.88 g, 0.76 mmol) and heated to 110 °C for 3.5 h. The resulting solution was cooled to 0 °C and carefully treated with H_2O_2 (30%, 10 mL). After warming to room temperature and stirring for an additional hour, the mixture was diluted with ether and washed successively with 2 N HCl and saturated aq NaCl. The organic layer was dried over Na_2SO_4, filtered, and concentrated. Purification by MPLC (10–100% ethyl acetate in heptane, 23 mL/min, 75 min) provided 6-fluoro-4-methoxy-biphenyl-3-carboxylic acid methyl ester (1.8 g, 91%) as a pale yellow solid: R_f 0.5 (40% ethyl acetate in heptane); ^{1}H NMR ($CDCl_3$, 300 MHz) δ 8.00 (d, J = 9.0 Hz, 1H), 7.53–7.33 (m, 5H), 6.79 (d, J = 12.6 Hz, 1H), 3.94 (s, 3H), 3.89 (s, 3H).

4.1.15. 6-Fluoro-4-methoxy-biphenyl-3-carboxylic acid (33). A solution of 6-fluoro-4-methoxy-biphenyl-3-carboxylic acid methyl ester (0.5 g, 2.3 mmol) in dioxane (8 mL, 0.3 M) was treated with 2 N NaOH (6.0 mL, 12 mmol) and stirred for 1 h at room temperature. The resulting reaction mixture was partially concentrated, acidified with 2 N HCl and extracted with ether. The organic layer dried over Na_2SO_4, filtered and concentrated to afford a 6-fluoro-4-methoxy-biphenyl-3-carboxylic acid (0.55 g, 96%) as a pale yellow powder: R_f 0.18 (5% methanol in dichloromethane); ^{1}H NMR ($CDCl_3$, 300 MHz) δ 8.35 (d, J = 9.0 Hz, 1H), 7.55–7.52 (m, 2H), 7.48–7.38 (m, 3H), 6.89 (d, J = 11.7 Hz, 1H), 4.12 (s, 3H).

Examples **58**, **59**, and **60** were prepared in a manner analogous to examples **6** and **8** except 2,4,5-trifluoro-benzoic acid and 2,4,6-trifluoro-benzoic acid were used in place of 2,4-difluoro-benzoic acid.

Examples **83** and **84** were prepared from 2-hydroxy-5-trifluoromethoxy-benzoic acid using the method described for examples **6** and **8**.

4.1.16. 2-Hydroxy-5-trifluoromethoxy-benzoic acid. Aq NaOH (35 mL, 5.8 M, 204 mmol) was combined with an aq silver nitrate solution (35 mL water, 2.9 M, 102 mmol) and stirred. The resulting suspension was cooled to 0 °C and treated with 2-hydroxy-5-trifluoromethoxy-benzaldehyde (10.0 g, 48.5 mmol) in several portions. After the addition was complete, the reaction was stirred an additional 10 min and filtered. The precipitate was washed with hot water and the combined washings were acidified to pH 1 with concd HCl. The resulting precipitate was collected by vacuum filtration, dissolved in ethyl acetate, and washed with saturated aq

NaCl. The solution was dried over Na_2SO_4, filtered, and concentrated to give 2-hydroxy-5-trifluoromethoxy-benzoic acid (9.8 g, 91%) as a white solid: R_f 0.38 (20% methanol in dichloromethane); ^1H NMR ($CDCl_3$, 300 MHz) δ 10.30 (br s, 1H), 7.79 (d, $J = 3.0$ Hz, 1H), 7.41 (dd, $J_1 = 9.3$ Hz, $J_2 = 3.0$ Hz, 1H), 7.05 (d, $J = 9.0$ Hz, 1H).

4.2. Pharmacology

4.2.1. Enzyme preparation. Recombinant human aldose reductase (hALR2) was overexpressed in *E. coli* using a T7 based expression system and purified using a metal affinity column.[35] The enzyme was precipitated in 3.5 M ammonium sulfate, 10 mM Tris–HCl buffer and 1 mM DTT. The enzyme was centrifuged at 10,000 rpm for 10 min at 4 °C and the pellet was resuspended to an approximate concentration of 10–15 mg protein/mL in $(NH_4)_2SO_4$ in NaH_2PO_4, pH 6.6. Protein content was determined using Coomassie Protein Assay reagent (Pierce, Rockford, IL). Aliquots were made and the enzyme was stored at −40 °C.

Recombinant human aldehyde reductase (hALR1) supplied by Dr. K. Gabbay (Baylor College of Medicine, Houston, TX) was prepared as previously described.[36] The enzyme was stored in 5 mM sodium phosphate, pH 7.4, and 0.1 mM EDTA at 4 °C. Protein content was determined using Coomassie Protein Assay reagent (Pierce, Rockford, IL).

4.2.2. Enzymatic assays. The method to examine the inhibition of aldose reductase (ALR2) was similar to those methods used by numerous other laboratories.[37–39] Enzymatic activity was measured by monitoring the disappearance rate of NADPH. Briefly, compound or solvent is placed in the microplate well to which buffer is added and mixed for 1 min. Enzyme is added to the well and incubated at 37 °C and shaken for 10 min. DL-Glyceraldehyde and NADPH are added to initiate the reaction. The microplate is placed in the platereader for 30 min at 340 nm and read at 2 min intervals. The reaction contents in a final volume of 300 μL are 6.6% $(NH_4)_2SO_4$, 33 mM NaH_2PO_4 (pH 6.6), 0.11 mM NADPH, 4.7 mM DL-glyceraldehyde, 0.59 μg enzyme, 1% DMSO, and compound. Percent inhibition is calculated based on the enzyme activity in the presence or absence of compound. The IC_{50} is calculated using SAS release 6.10 and a four-parameter logistic regression of data.

The inhibition of aldehyde reductase (ALR1) was assessed using a standard spectrophotometric assay.[36] The procedure is similar to the method described above for determining ALR2 inhibition. The reaction contents in a final volume of 300 μL are 33 mM NaH_2PO_4 (pH 6.6), 0.11 mM NADPH, 4.7 mM DL-glyceraldehyde, 0.28 μg enzyme, 1% DMSO, and compound.

4.2.3. STZ-induced diabetic rat model. Male Sprague–Dawley rats (Harlan, Indianapolis, IN), weighing 150 g, are allowed to acclimate for one week and placed on a standard diet (7012, Harlan Teklad certified LM-485 mouse/rat, Madison, WI). Water is supplied ad libitum. After a 24 h fast, 40 mg/kg STZ (S01230 Sigma, St. Louis, MO) prepared in 0.03 M citrate buffer, pH 4.5 is administered ip. Control animals receive citrate buffer.

Four days after receiving STZ, tail blood glucose is measured using a One Touch II blood glucose meter (Lifescan, Inc., Johnson & Johnson, Milpitas, CA). Diabetic rats whose blood glucose levels are $\geqslant 300$ mg/dl are randomized according to blood glucose levels into diabetic control and diabetic-treatment groups. Each study includes 5 nondiabetic controls, 10 diabetic controls, and 7 diabetic rats for each drug-treated group.

Beginning on day 4 after induction of diabetes with STZ, the compound is administered for five consecutive days po suspended in a vehicle of 2% Tween 80 in saline. Nondiabetic and diabetic controls receive vehicle during this period. After the initial dose of compound, animals continue to receive the standard diet for the remainder of the study. After receiving the final dose of compound, the food is removed. Four hours after the final dose is administered, the rats are euthanized by asphyxiation with CO_2 and sciatic nerves are removed, weighed, frozen on porcelain plates on dry ice, and stored at −80 °C for sorbitol analysis.

4.2.4. Tissue sorbitol analysis. Sciatic nerve sorbitol levels are measured by a standard enzymatic method that uses sorbitol dehydrogenase.[40,41] A D-sorbitol kit purchased from Boehringer Mannheim (670 057 Indianapolis, IN) was adapted to a microplate format.

Tissues are homogenized in ice cold 0.2% perchloric acid in methanol using a DUALL tissue grinder and centrifuged at 10,000 rpm for 10 min at 4 °C. A sampling of the supernatant is transferred to a microplate. A reaction mixture combining buffer, diaphorase, NAD^+, and iodonitrotetrazolium chloride (INT) is added to each sample followed by an initial absorbance reading at 490 nm. Sorbitol dehydrogenase (SDH) is added to initiate the reaction and the plate is mixed for 90 s on an orbital shaker. Plates are incubated at room temperature in the dark for 30 min and the final absorbance reading at 490 nm is made. The reaction contents in a final volume of 255 μL at pH 8.7 are 14.1 mM potassium phosphate, 94 mM triethanolamine, 0.94% Triton X-100, 0.16 U diaphorase, 1.66 mM NAD, 0.034 mM INT and 0.82 U SDH.

Sciatic nerve sorbitol content is calculated as nmol sorbitol/mg wet tissue weight by taking the difference in the final and initial absorbance readings and comparing to a sorbitol standard curve. % Inhibition is calculated by comparing treatment groups to both the nondiabetic and diabetic control groups within the study as described by the equation: $(t - n)/(d - n)$ where n = nondiabetic control, d = diabetic control, and t = drug-treated diabetic control. The ED_{50} was calculated using Sigma plot, version 4.0, using a Hill slope four-parameter logistic equation.

4.3. X-ray crystallography

4.3.1. Overproduction and purification of recombinant human ALR2. The ORF of the human ALR2 gene (Accession GenBankTM/embl Data Bank Number J05017) was amplified by PCR from its cDNA and cloned into the T7 RNA polymerase-based vector pET15b (Novagen). Expression of the (HIS)6-human ALR2 in the *E. coli* strain BL21(DE3) (Novagen) is induced by IPTG (Euromedex) during a 3 h culture at 37 °C. The pellet from a 4 L culture was disrupted by sonication and centrifuged at 4 °C. The supernatant was applied on a Talon metal affinity column (Clontech). After thrombin cleavage of the hexahistidine extension, the detagged protein was then loaded on a DEAE Sephadex A-50 column (Pharmacia) and eluted with a NaCl gradient.

4.3.2. Crystallization trials and preliminary crystallographic analysis. All trials were carried out in Linbro 24-well tissue culture plates (Flow Laboratories) using the hanging-drop vapor diffusion method. The enzyme was dialyzed against 50 mM ammonium citrate pH 5.0. The drops of a final volume of 12 mL contained 15 mg/mL of human ALR2 with 2 equiv of $NADP^+$ (Sigma) and 5% of PEG 6000; they were equilibrated against a well containing 120 mM ammonium citrate, pH 5.0, 20% PEG 6000 and the same concentration of $NADP^+$ as above. Crystals were grown at 4 °C and reached the size of $0.5 \times 0.4 \times 0.4$ mm.

4.3.3. Soaking with the inhibitor. Crystals of the ALR2-inhibitor complex were obtained by soaking of the native crystals with a solution containing 2 mg/mL of inhibitor dissolved in the mother liquor containing 120 mM ammonium citrate, pH 5.0, and 25% of PEG 6000. The soaking time was three weeks.

4.3.4. Data collection and refinement. The diffraction analysis was performed using a rotating anode laboratory source and an image plate, and the data treated with the HKL package.[42] The inhibitor-soaked crystals diffracted to 1.8 Å and were isomorphous to the native crystals. The native structure was used as a model for the molecular replacement; after a rigid-body minimization, the inhibitor was placed in the electron density shown by a Fourier difference map. The model of the complex was used as starting point of the refinement, which included a rigid-body refinement step, a slow-cooling step, a Powell minimization, and a temperature-factor refinement. Water molecules were then placed in a difference map and minimization was performed as above without putting restraints on the water molecules; bulk solvent correction was also applied. The programs O[43] and X-PLOR[44] were used for model building and refinement.

Diffraction experiments were conducted on two crystals at the X-ray beam of the undulator line 19ID of SBC-CAT at the APS. All conditions were optimized for the high resolution experiments.[29]

The atomic coordinates and structure factors of the hALR2-$NADP^+$-example **40** (IDD 594) complex have been deposited in the Protein Data Bank (1US0).

Acknowledgements

This work was supported, in part, by the Centre National de la Recherche Scientifique (CNRS), the Institut National de la Santé et de la Recherche Médicale and the Hôpital Universitaire de Strasbourg (H.U.S.). We thank the personnel of the SBC, and in particular Andrzej Joachimiak and Ruslan Sanishvili (Nukro), for their help in data collection.

Supplementary data

Supplementary data associated with this article can be found, in the online version, at doi:10.1016/j.bmc.2004.07.062.

References and notes

1. American Diabetes Association's homepage. http://www.diabetes.org.
2. The Diabetes Control and Complications Trial Research Group. The effect of intensive treatment of diabetes on the development and progression of long-term complications in insulin-dependent diabetes mellitus. *New Engl. J. Med.* **1993**, *329*, 977–986.
3. The United Kingdom Prospective Diabetes Study Group. Intensive blood–glucose control with sulfonyl-ureas or insulin compared with conventional treatment and risk of complications in patients with type 2 diabetes (UKPDS33). *Lancet* **1998**, *352*, 837–853.
4. *Textbook of Diabetes*; Pickup, J. C., Williams, G., Eds.; Blackwell Science: United Kingdom, 1997; Vol. 1, Chapter 42.
5. Williamson, J. R. et al. Hyperglycemic pseudohypoxia and diabetic complications. *Diabetes* **1993**, *42*, 801–813.
6. Lee, A.; Chung, S. K.; Chung, S. S. Demonstration that polyol accumulation is responsible for diabetic cataract by use of transgenic mice expressing the aldose reductase gene in the lens. *Proc. Natl. Acad. Sci. U.S.A.* **1995**, *92*, 2780–2784.
7. Oates, P. J.; Mylari, B. L. Aldose reductase inhibitors: therapeutic implications for diabetic complications. *Expert Opin. Inv. Drug.* **1999**, *8*, 1–15.
8. Kao, Y.-L.; Donahue, K.; Chan, A.; Knight, J.; Silink, M. A novel polymorphism in the aldose reductase gene promoter region is strongly associated with diabetic retinopathy in adolescents with Type I diabetes. *Diabetes* **1999**, *48*, 1338–1340.
9. Heesom, A.; Hibberd, M.; Millward, A.; Demaine, A. Polymorphism in the 5′-end of the aldose reductase gene is strongly associated with the development of diabetic nephropathy in Type I diabetes. *Diabetes* **1997**, *46*, 287–291.
10. Moczulski, D. et al. The role of aldose reductase gene in the susceptibility to diabetic nephropathy in Type II (non-insulin-dependent) diabetes mellitus. *Diabetologia* **1999**, *42*, 94–97.
11. Shinoda, M.; Mori, S.; Shintani, S.; Ishikura, S.; Hara, A. Inhibition of human aldehyde reductase by drugs for testing the function of liver and kidney. *Biol. Pharm. Bull.* **1999**, *22*, 741–744.
12. Suzuki, K.; Koh, Y. H.; Mizuno, H.; Hamaoka, R.; Taniguchi, N. Overexpression of aldehyde reductase

protects PC12 cells from the cytotoxicity of methylglyoxal or 3-deoxyglucosone *J. Biochem.* **1998**, *123*, 353–357.
13. Takahashi, M.; Fujii, J.; Teshima, T.; Suzuki, K.; Shiba, T.; Taniguchi, N. Identity of a major 3-deoxyglucosone-reducing enzyme with aldehyde reductase in rat liver established by amino acid sequencing and cDNA expression. *Gene* **1993**, *127*, 249–253.
14. Kanazu, T.; Shinoda, M.; Nakayama, T.; Deyashiki, Y.; Hara, A.; Sawada, H. Aldehyde reductase is a major protein associated with 3-deoxyglucosone reductase activity in rat, pig and human livers. *Biochem. J.* **1991**, *279*, 903–906.
15. Hamada, Y.; Araki, N.; Koh, N.; Nakamura, J.; Horiuchi, S.; Hotta, N. Rapid formation of advanced glycation end-products by intermediate metabolites of glycolytic pathway and polyol pathway. *Biochem. Biophys. Res. Commun.* **1996**, *228*, 539–543.
16. Oya, T.; Hattori, N.; Mizuno, Y.; Miyata, S.; Maeda, S.; Osawa, T.; Uchida, K. Methylglyoxal modification of protein. *J. Biol. Chem.* **1999**, *274*, 18492–18502.
17. Cavalot, F.; Anfossi, G.; Russo, I.; Mularoni, E.; Massucco, P.; Mattiello, L.; Burzacca, S.; Hahn, A.; Trovati, M. Nonenzymatic glycation of fibronectin impairs adhesive and proliferative properties of human vascular smooth muscle cells. *Metabolism* **1996**, *45*, 285–292.
18. Fu, M.; Wells-Knecht, K.; Blackledge, J.; Lyons, T.; Thorpe, S.; Baynes, J. Glycation, glycoidation, and cross-linking of collagen by glucose. *Diabetes* **1994**, *43*, 676–683.
19. Flynn, T. G.; Green, N. C.; Bhatia, M. B.; El-Kabbani Structure and mechanism of aldehyde reductase. In *Enzymology and Molecular Biology of Carbonyl Metabolism 5*; Weiner, et al., Eds.; Plenum: New York, 1995; Chapter 25, pp 193–201.
20. Harrison, D. H. T.; Bohren, K. M.; Petsko, G. A.; Ringe, D.; Gabbay, K. H. The alrestatin double-decker: binding of two inhibitor molecules to human aldose reductase reveals a new specificity determinant. *Biochemistry* **1997**, *36*, 16134–16140.
21. Umezu, K. Preparation of 4-fluorosalicylic acids from difluorobenzoic acids in polar aprotic solvents. Japanese patent JP 96-193878.
22. Wrobel, J.; Millen, J.; Sredy, J.; Dietrich, A.; Gorham, B.; Malamas, M.; Kelly, J.; Bauman, J.; Harrison, M.; Jones, L.; Guinosso, C.; Sestanj, K. Synthesis of tolrestat analogues containing additional substituents in the ring and their evaluation as aldose reductase inhibitors. Identification of poten, orally active 2-fluoro derivatives. *J. Med. Chem.* **1991**, *34*, 2504–2520.
23. Hartwell, J. L. *o*-Chlorobromobenzene. *Org. Syn. (Collective Volume III)*, **1955**, 185.
24. Wolfe, J.; Büchwald, S. Scope and limitations of the Pd/BINAP-catalyzed amination of aryl bromides. *J. Org. Chem.* **2000**, *65*, 1144–1157.
25. Urzhumtsev, A.; Tête-Favier, F.; Mitschler, A.; Barbanton, J.; Barth, P.; Urzhumtseva, L.; Biellmann, J.-F.; Podjarny, A. D.; Moras, D. A. 'Specificity' pocket inferred from the crystal structures of the complexes of aldose reductase with the pharmaceutically important inhibitors tolrestat and sorbinil. *Structure* **1997**, *5*, 601–612.
26. El-Kabbani, O.; Wilson, D. K.; Petrash, J. M.; Quiocho, F. A. Structural features of the aldose reductase and aldehyde reductase inhibitor-binding sites. *Mol. Vis.* **1998**, *4*, 19–25.
27. Rees-Milton, K. J.; Jia, Z.; Green, N. C.; Bhatia, M.; El-Kabbani, O.; Flynn, T. G. Aldehyde reductase: the role of C-terminal residues in defining substrate and cofactor specificities. *Arch. Biochem. Biophys.* **1998**, *355*, 137–144.
28. El-Kabbani, O.; Carper, D. A.; McGowan, M. H.; Devedjiev, Y.; Rees-Milton, K. J.; Flynn, T. G. Studies on the inhibitor-binding site of porcine aldehyde reductase: crystal structure of the holoenzyme-inhibitor ternary complex. *Proteins* **1997**, *29*, 186–192.
29. Howard, E.; Sanishvili, R.; Cachau, R.; Mitschler, A.; Chevrier, B.; Barth, P.; Lamour, V.; Van Zandt, M. C.; Sibley, E.; Bon, C.; Moras, D.; Schneider, T. R.; Joachimiak, A.; Podjarny, A. Ultrahigh resolution drug design I: details of interactions in human aldose reductase-inhibitor complex at 0.66 Å. *Proteins: Struct., Funct., Bioinformatics* **2004**, *55*, 792–804.
30. Kotani, T.; Nagaki, Y.; Ishii, A.; Konishi, Y.; Yago, H.; Suehiro, S.; Okukado, N.; Okamoto, K. Highly selective aldose reductase inhibitors. 3. Structural diversity of 3-(arylmethyl)-2,4,5-trioxoimidazolidine-1-acetic acids. *J. Med. Chem.* **1997**, *40*.
31. Malamas, M.; Holman, T.; Millen, J. Novel spirosuccinimide aldose reductase inhibitors derived from isoquinoline-1,3-diones: 2-[(4-bromo-2-fluorophenyl)methyl]-6-fluorospiro[isoquinoline-4(1H),3′-pyrrolidine]-1,2′,3,5′(2H)-tetrone and congeners. *J. Med. Chem.* **1994**, *37*, 2043–2058.
32. Mylar, B.; Larson, E.; Beyer, T.; Zembrowski, W.; Aldinger, C.; Dee, M.; Siegel, T.; Singleton, D. Novel, potent aldose reductase inhibitors: 3,4-dihydro-4-oxo-3-[[5-(trifluoromethyl)-2-benzothiazolyl]methyl]-1-phthalazine-acetic acid (zopolrestat and congeners). *J. Med. Chem.* **1991**, *34*, 108–122.
33. Jones, M.; Gunn, D.; Jones, J.; Van Zandt, M. U.S. Patent 6,214,991, 2001.
34. Tomoji, A.; Nishio, T.; Hosono, H.; Nakamura, Y.; Matsui, T.; Ishikawa, H. U.S. Patent 5,543,420, 1994.
35. Hayman, S.; Kinoshita, J. H. *J. Biol. Chem.* **1965**, *240*, 877–880.
36. Barski, O. A.; Gabbay, K. H.; Grimshaw, C. E.; Bohren, K. M. Mechanism of human aldehyde reductase: characterization of the active site pocket. *Biochemistry* **1995**, *34*, 11264–11275.
37. Stribling, D.; Mirrlees, D. J.; Harrison, H. E.; Earl, D. C. N. Properties of ICI 128,436 a novel aldose reductase inhibitor, and its effects on diabetic complications in the rat. *Metabolism* **1985**, *4*, 336–344.
38. Ashizawa, N.; Yoshida, M.; Sugiyama, Y.; Akaike, N.; Ohbayashi, S.; Aotsuka, T.; Abe, N.; Fukushima, K.; Matsuura, A. Effects of a novel potent aldose reductase inhibitor, GP-1447, on aldose reductase activity in vitro and on diabetic neuropathy and cataract formation in rats. *Jpn. J. Pharmacol.* **1997**, *73*, 133–144.
39. Ehrig, T.; Bohren, K. M.; Prendergast, G.; Gabbay, K. Mechanism of aldose reductase inhibition: binding of $NADP^+$/NADPH and alrestatin-like inhibitors. *Biochemistry* **1994**, *33*, 7157–7165.
40. Bergmeyer, H. U.; Gruber, W.; Gutmann, I. In *Methods of Enzymatic Analysis*, 2nd ed.; Bergmeyer, H. U., Ed.; Weinheim and Academic: New York, London, 1974; Vol. 3, pp 1323–1330.
41. Malone, J. I.; Knox, G.; Benford, S.; Tedesco, T. A. Red cell sorbitol. An indicator of diabetic control. *Diabetes* **1980**, *29*, 861–864.
42. Otwinowski, Z.; Minor, W. In *Methods in Enzymology, Macromolecular Crystallography, part A*; Carter, C. W., Jr., Sweet, R. M., Eds.; Academic, 1997; Vol. 276, pp 307–326.
43. Jones, T. A.; Zou, J. Y.; Cowan, S. W.; Kjeldgaard, M. O. *Acta Cryst.* **1991**, *A47*, 110–119.
44. Brunger, A. T. Yale University Press: New Haven, CT, USA, 1992.